AN INTEGRATED ANAEROBIC-PHOTOCATALYTIC-MAGNETIC WASTEWATER TREATMENT SYSTEM

Emmanuel Kweinor Tetteh and Sudesh Rathilal

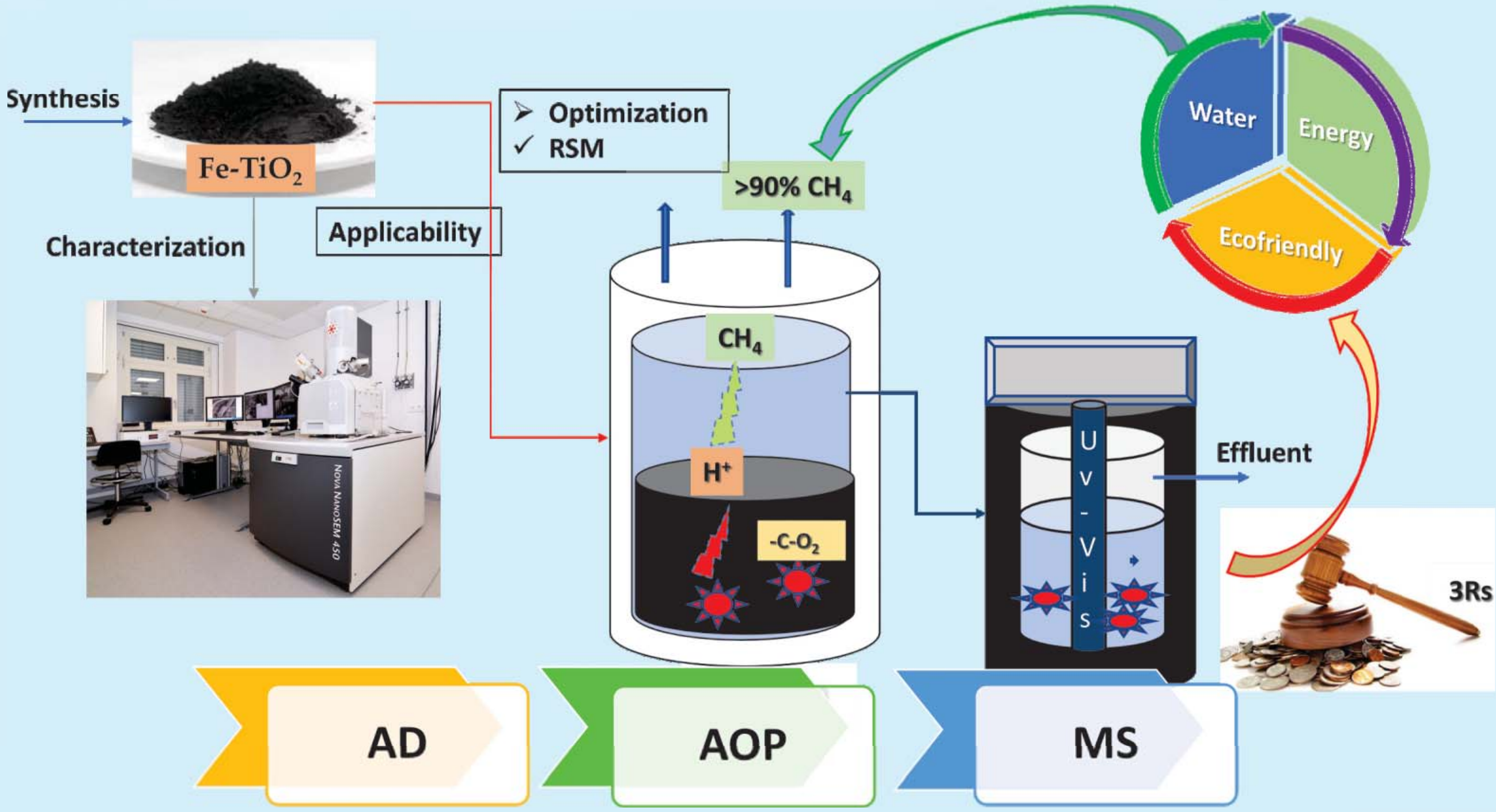

WATER RESEARCH COMMISSION

TT 901/22

AN INTEGRATED ANAEROBIC-PHOTOCATALYTIC-MAGNETIC WASTEWATER TREATMENT SYSTEM

Report to the
Water Research Commission

by

Emmanuel Kweinor Tetteh
(Principal investigator)

Sudesh Rathilal
(Project leader)

Green Engineering Research Group
Department of Chemical Engineering
Durban University of Technology

WRC Report No. TT 901/22

ISBN 978-0-6392-0457-4

February 2023

WATER
RESEARCH
COMMISSION

Obtainable from
Water Research Commission
Lynnwood Bridge Office Park
Bloukrans Building
4 Daventry Road
Lynnwood Manor
PRETORIA

orders@wrc.org.za or download from www.wrc.org.za

This is the final report of WRC project no. C2019/20-00212

DISCLAIMER

This report has been reviewed by the Water Research Commission (WRC) and approved for publication. Approval does not signify that the contents necessarily reflect the views and policies of the WRC, nor does mention of trade names or commercial products constitute endorsement or recommendation for use.

Executive summary

Wastewater treatment plants in South Africa's municipalities are currently being challenged by the presence of emerging contaminants in wastewater, and this impacts the costs of the treatment process. Conventionally, treatment of municipal wastewater involves a sequence of treatment units aimed at reducing pollutants to acceptable discharge levels. However, the current treatment approach does not address the presence of emerging contaminants in wastewater as well as present significant opportunities for wastewater valorisation. There is, therefore, a need for the development of sustainable wastewater treatment technologies. This study aimed to develop an integrated anaerobic digestion-advanced oxidation photocatalytic (AD-AOP) magnetized system for the valorisation of industrial wastewater into bioenergy.

To obtain an optimal balance between robustness and cost-effectiveness of the integrated system, the applicability performance of the magnetized photocatalysts (MPCs) was explored. In terms of energy production and utilisation, the cost-benefit analysis and treatability efficiency of the integrated system was evaluated. Furthermore, using the best MPC, the kinetic modelling and optimisation of the integrated process was carried out to ascertain its treated wastewater energy potential and CO_2 emission reduction. Herein, the response surface methodology was employed for the experimental design, data evaluation and modelling. The wastewater samples used in this project were obtained from Umgeni water, eThekwini municipality, and local sugar and oil refinery industries located in KwaZulu-Natal. The water quality parameters of the effluent measured to determine the treatability efficiency included chemical oxygen demand (COD), total suspended solids (TSS), volatile suspended solids (VSS), total solids (TS), pH, nitrites (NO_2), nitrates (NO_3) and total ammonia nitrogen (NH_3-N).

The characterization of the synthesized binary (Fe-TiO_2) and ternary (Fe/Ch-TiO_2 and Fe/Al-TiO_2) MPCs carried out via a co-precipitation technique suggested that they were successfully magnetized. This was further validated by using Scanning Electron Microscopy (SEM) and Energy Dispersive X-Ray (EDX), Fourier Transformation Infrared (FTIR) spectra, X-Ray Diffraction (XRD) and Brunauer-Emmett-Teller (BET) techniques. To establish the environmental trade-off of the MPCs and treatability potential, a series of their applicability was carried out with biological and photocatalytic systems. Among the MPCs, Fe-TiO_2 with high surface area (63 m^2/g), pore volume (0.02 cm^3/g) and pore size (1.3 nm) were found to exhibit the best performance.

In terms of the technological development and evaluation, a series of engineering works in biochemical methane potential (BMP) tests, bio-photocatalytic (BPs), bio-magnetic (BMs) and biophotomagnetic (BPMs) systems were explored. The integrated AD-AOP magnetized system showed great potential for the recoverability of the MPCs for reuse; reducing toxicological effects of trace metals (27 elements considered) and improving water and biogas quality in the wastewater settings. This resulted in more than 75% color, chemical oxygen demand (COD) and turbidity removal.

The integrated system's experimental design, process optimization and modelling were done via the RSM-Box-Behnken design (BBD). At RSM-BBD optimal conditions of OLR (0.394 kgCOD/Ld.), HRT (20 d) and AOP with a UV-light irradiation source (98.96 kWh/L used), 1250 mL/d of biogas equating to 38.02 kWh/L bioenergy, 99% COD removal, net energy efficiency of 38.43% and CO_2 emission reduction of 10859.5 kgCO_2e/L were estimated. The experimental validity was in good agreement with the model predicted results at high regression values (R^2 >0.98) and 95% confidence levels.

Overall, the study findings provide an insight into the synthesis and applicability of MPCs, kinetics and RSM modelling and optimization as a potential to develop an optimized integrated AD-AOP magnetized system towards the treatment of industrial wastewater coupled with biogas generation and CO_2 emission reduction. The study outcomes therefore warrant further development on upscaling the integrated system to a pilot study that will also include smart-online monitoring systems in support of improved wastewater valorization. Also, the synthesis of magnetized nanomaterials has great potential for commercialization and industrial applications.

Graphical abstract

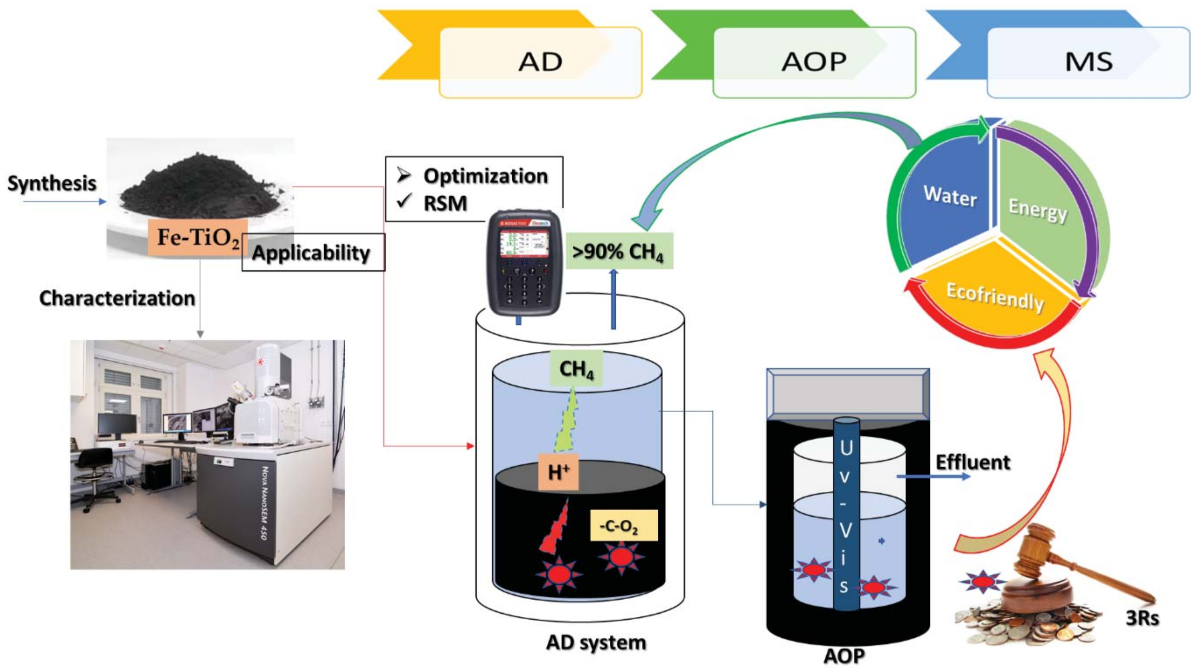

Acknowledgements

We acknowledge the support, advice and thought-provoking discussions instigated by the WRC Reference Group members listed below. Your contribution and commitment helped us achieve the goals of the project. We also appreciate Dr Dennis Isaac Amoah (DUT, Institute for Water and Wastewater Technology), the DUT Green Engineering research group members, which includes Dr Martha Noro Chollom, Ms Gloria Amo-Duodu and Ms Nomthandazo Sibiya for their valuable involvement and dedication to this project. Our profound thanks to Mr Jaafar Mohammed Bux and Ms Seshna Sewsanker at DUT, Department of Chemical Engineering labs. Special thanks to iThemba labs and Miss Miranda Waldron (University of Cape Town) for their respective help for the XRD and SEM/EDX sample characterisation. Our sincere appreciation goes to Mr Sam Donyina (Work Superintendent at Umbilo eThekweni Water Works) and staff at Umgeni Water PMB and FFS Refiners for assisting us with the samples.

Reference group members:

Prof JN Zvimba (Water Research Commission – Chairperson)

Mr Benny Mokgonyana (WRC Project Administrator: Research & Development)

Prof VL Pillay (Stellenbosch University)

Mr MO Mnguni (Umgeni Water)

Mr M Cele (eThekwini Municipality)

Mr A Canning (Industry)

Prof PO Osifo (Vaal University of Technology)

Dr MR Chowdhury (Cape Peninsula University of Technology)

Mr AJ Steytler (Industry)

Dr BO Otieno (Vaal University of Technology)

Dr SO Apollo (Vaal University of Technology)

Capacity building

The Doctoral and Masters students listed below are currently actively involved in this ongoing WRC project (C2019/2020-00212) and are benefiting through stipends, conference funding and purchasing of equipment, chemicals and consumables. The listed BTech students also worked on research projects which are only related to this project and their running costs were partly paid by this project. The Research Assistant is currently co-supervising one of the Masters projects, whereas the Masters students were actively involved in supervising the BTech projects. The Doctoral student was the lead investigator and was actively involved in all the Masters and BTech projects as well as his own Doctoral study.

Mr Emmanuel Kweinor Tetteh (DEng-2022) – Ghanaian

Dr Martha Noro Chollom (Research Assistant) – Nigerian

Ms Gloria Amo-Duodu (MEng-2022) – Ghanaian

Ms Nomthandazo Sibiya (MEng-2022) – South African

Ms T Pillay (BTech-2020) – South African

Mr P Govender (BTech-2020) – South African

Ms Mbole Mbuyu (BTech-2020) – South African

Ms Buthelezi Khana Sthembile (BTech-2021) – South Africa

Ms Thakhani Tshifhango (BEngHons-2021) – South Africa

Publications – Journal and Conference Papers

Aside this report, 18 articles have been published in peer reviewed journals, 4 submitted and 3 are in preparation for submission. Also, a total of 18 presentations were done at both local and international conferences in order to disseminate valuable information from this project.

Table of Contents

Chapter 1: Introduction

1.1 Background

Rapid urbanization and industrialization have increased the demand for wastewater treatment in metropolitan areas, whereas upgrading and expansions of water supply systems is inevitable. In essence, wastewater pollution endangers human health and the aquatic ecology, making it one of the world's biggest environmental issues today (Sahani et al., 2022). Herein, the development of centralised wastewater treatment systems, which is energy efficient to mitigate emerging contaminants (ECs) and environmental challenges associated with the water sector is globally gaining attention (Adetunji and Olaniran, 2021; Divyapriya et al., 2021). However, diversity of wastewater resources is not only associated with the industries (textile, refining, mining, agrochemical, pharmaceutical, pulp and paper, food industry, etc.) that generate them, but also the concentration level of the contaminants (Marcoux et al., 2013; Adetunji and Olaniran, 2021).

Generally, water-soluble substances are easier to be distributed and transported in the water cycle and their direct impact in the ecosystem can be noticed within a short possible time (Riaz and Park, 2020; Tetteh et al., 2020a). However, advancement of scientific environmental assessments reveals recalcitrant ECs (antibiotics, COVID-19 RNA, pesticides, nanomaterials, endocrine disruptors, solvents) (Diamadopoulos et al., 2007; Chollom et al., 2020a), after a long period can still be detected in the wastewater streams (Chollom et al., 2020a). As result, high levels of toxic organic matter and heavy metals without proper treatment poses great threats to human life and the ecosystem along with sub operational issues of most water and wastewater treatment plants (WWTPs) (Marcoux et al., 2013; South African-German Energy Programme (GIZ-SAGEN, 2015). Some of these wastewater pollutants include total dissolved solids (TDS), total suspended solids (TSS), biological oxygen demand (BOD), chemical oxygen demand (COD), total phosphorus, nitrates and nitrites, faecal coliforms and so on. This has drawn attention of many stakeholders in the water sector to improve the efficacy of WWTPs.

In South Africa, treated effluents continue to degrade most inland raw water sources (Momba and Swartz, 2010). This causes eutrophication, which leads to excessive algal growths that have detrimental impacts on water quality, such as the generation of algae toxins and odour-causing compounds and precursors that produce halogenated by-products (e.g. trihalomethanes) upon chlorination. Algae in raw water also hinders physical separation techniques used to remove algae during treatment (Goswami et al., 2021). Furthermore, the recent societal and industrial activity reliance on fossil fuels and water demand have intensified environmental problems. These problems directly undermine the United Nations (UN, 2015) Sustainable Development Goals (SDGs) especially those associated with clean water and sanitation (SDG 6), health (SDG 3), and sustainable management of waste (SDG 11) as well as clean and affordable energy (SDG 7). Consequently, the South Africa Department of Water Affairs developed the National Water Resource Strategy (NWRS) II in June 2013, intending to ensure equitable and sustainable access to and use of water for all South Africans while also safeguarding the country's water resources. According to the same NWRS report, an investment of around R700 billion is required in the near future to address the technical requirements of the affected water value chain (Van Niekerk and Schneider 2013).

Anaerobic digestion (AD) of wastewater offers great potential for recovering energy (biogas) as a renewable source of energy from wastewater, where the presence of biorecalcitrant contaminants becomes a threat. Conventionally, AD is insufficient to handle high EC water supply and quality concerns and therefore warrants advanced technologies. Membrane filtration (microfiltration, ultrafiltration, nanofiltration, and reverse osmosis) and/or advanced oxidation processes (AOP) are commonly used as a polishing step to minimise natural organic matter from wastewater streams. In terms of waste disposal and further treatment, AOP heterogeneous photocatalysts offer more advantages than membrane filtration due to rapid conversion reactions, such as mineralizing hazardous contaminants to harmless compounds like carbon dioxide (CO_2), water (H_2O), simple acids and salts. AOP can use sunlight as a clean energy supply to reduce environmental pollution and employs ambient oxygen rather than expensive oxidants like hydrogen peroxide and ozone. In view of this, AOPs have many setbacks, including difficulty to recover the photocatalyst and its energy driven tenacity makes it expensive to operate (Della Rocca et al., 2021; Bica et al., 2022).

Moreso, metal oxide nanoparticles, such as titanium dioxide (TiO_2), aluminium oxide (Al_2O_3), silicon dioxide (SiO_2), and zinc oxide (ZnO), have received increasing interest due to their industrial applications in the water sector (Chong et al., 2010; Xu et al., 2019; Adetunji and Olaniran, 2021). Among them, TiO_2 as semiconductive nanoparticles can generate reactive oxygen species (ROS) such as free radicals (OH*, H*), that can rupture cell walls and damage ECs. However, intentional, or unintentional release of these nanoparticles into the environment may affect human health, soil, and aquatic organisms. As the specific mechanism of toxicity for nanoparticle exposure is not entirely understood, their application in large scale therefore warrants toxicity evaluation, recoverability modification, safe disposal of wastes and energy saving efficiency. On this basis, incorporating a magnetised TiO_2 photocatalyst (Fe-TiO_2) with high surface-volume ratio and magnetic properties is seen to have great potential for magnetic separation technology in the wastewater settings. Notwithstanding, the usage of energy and water are closely related, as energy is the driving force of water distribution systems. So, improving water-energy efficiency by introducing magnetised nanomaterials into water treatment systems come in handy.

Against this background, transforming the sewage management sector in South Africa into renewable energy source will necessitate the development of wastewater treatment technologies with sustainable benefits. On this premise, this project aimed to develop an integrated anaerobic-photocatalytic-magnetized wastewater treatment system as a viable wastewater remediation alternative. Additionally, integrating AD and AOP provides a sustainable alternative solution for offsetting the AOP energy demand with biogas produced by the AD system, while the magnetised system facilitates the recovery of Fe-TiO_2 nanoparticles. Herein, to transform this lab-scale integrated system into a more sustainable system warrants process optimisation and implementation strategies. However, the geometrical, and operational parameters that govern the dynamics of the system performance have complex interactive effects. Therefore, in evaluating the relevant operational factors and their complex interactions, response surface methodology (RSM) was employed as a computational prediction and validation tool of the experimental data.

1.2 Aim and objectives.

This project aimed to develop an integrated AD-AOP magnetized system for treatment and valorisation of industrial wastewater. The specific objectives are outlined as:

1. Synthesis and characterisation of the TiO_2 magnetized photocatalyst (MPC) for industrial wastewater treatment and biogas enhancement
2. Design, monitoring and evaluation of the lab-scale integrated anaerobic-photo-catalytic-

magnetic system for municipality wastewater treatment

3. Modelling and optimising the integrated AD-AOP magnetised system for municipality wastewater treatment with estimated energy produced and CO_2 emission reduction.

Aside this scope, this project is expected in the future, to develop a smart integrated AD-AOP magnetized system for the abatement of wastewater as useful resources for biogas generation as a sustainable wastewater management system in South Africa.

Chapter 2: Literature review on AD-AOP systems

2.1 Overview of wastewater treatment

To achieve stringent discharge limits, WWTPs use a variety of physical-chemical and biological processes to purify the water. Within this context, most of the polluting compounds that are predominantly eliminated from the treated water lie within the range of micro- and nano-scale particles. This involves the elimination of pathogenic viruses, monovalent ions (Na^+ and Cl^-), hardness producing ions (Ca^{2+} and Mg^{2+}), colloids/turbidity, and organic contaminants that cause taste and odour problems (Lamichhane et al., 2022; Lu et al., 2007). In addition, the burden of suspended pollutants from non-point sources is increasing due to the diverse forms of ECs, which is leading to poor water quality and sanitation (Sahani et al., 2022; Sivaranjanee and Kumar, 2021).

To lessen the severity of this problem, a viable technology that integrates different treatment technologies is encouraged. Notwithstanding, conventional WWTPs may consist of primary (physio-chemical processes involving coagulation/sedimentation), secondary (AD, activated sludge digesters or trickling filters) and tertiary (filtration, chlorination, disinfection), as well as advanced processes (photocatalysis, membrane filtration and adsorption) (Stafford et al., 2013; Kweinor Tetteh et al., 2019; Ponce-Robles et al., 2020). The biological methods including anaerobic (absence of oxygen) and aerobic (oxygen present) systems are commonly engineered to boost biochemical degradation of the organic content of the wastewater (Dan Eddy, 2003). The biodegradation by fungi, bacteria and algae have been the main route through which large molecular compounds including biodegradable ECs are broken down into simpler substances. According to Göbel et al. (2007), the removal rates by biological process are usually within the range 20 to 65% and in some cases lesser than that are observed. As a result, advanced and tertiary methods have found great application in WWTPs, especially in cases where high quality effluent is required for reuse purposes. These methods are used as a polishing step or post-treatment to a secondary effluent. They have the capability to degrade organic matter and ECs above 65% and, in some instances, complete mineralisation can take place. The combination of AD with physio-chemical methods such as adsorption, coagulation/flocculation, and membrane separation have also been reported. However, the applicability of some of these processes comes with technological constraints including, capital and energy intensive costs, slow kinetics, irreversible adsorption of target compounds and loss of mechanical stability. So, to meet stringent discharge limits and treat wastewater for reuse warrants a combination of cost-effective treatment technologies (Lakshmanan, 2013; Naldoni et al., 2019). Therefore, presented in Figure 1 is the benchmark strategy which was adapted in this study for the selection of the appropriate integrated technology for the valorisation of the wastewater into bioenergy.

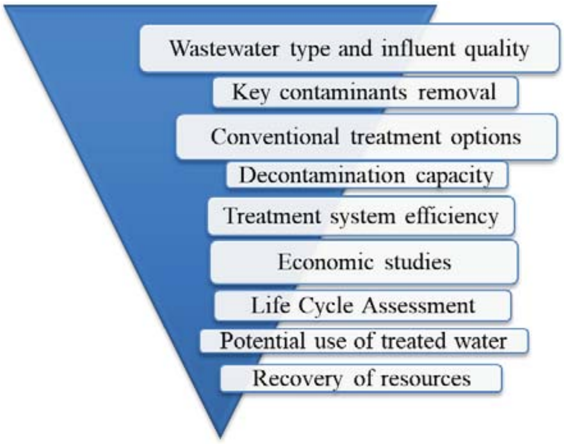

Figure 1: Schematic diagram of factors to be considered in selecting wastewater treatment technologies; Adapted from Fermoso et al. (2019)

2.2 Survey of integrated wastewater treatment systems

In South Africa, water quality monitoring, particularly for drinking water and wastewater are being driven by the legislature (The National Water ACT 36 of 1998). Bourgin et al. (2018) reported that the South African Water Act was introduced with an objective to improve water quality to meet reuse standards as a way of easing the water stressed regions. Also, the South African National Standards (SANS 241, 2015) are commonly applied to guarantee that drinking water quality is health risk free for South Africans. Currently, policies regarding the quality of effluent from WWTPs for discharge is becoming more stringent (Son et al., 2020). This necessitates existing WWTPs to implement an advanced post-treatment step for micro-pollutant abatement after the conventional treatment processes. Table 1 shows some extensive research on the feasibility and effectiveness of integrating biological and AOP systems (Gimeno et al., 2016; Paździor et al., 2019).

Table 1: Survey on anaerobic digestion and advanced oxidation process

(Wastewater) Pollutants degraded	**Biological treatment**	**Advance oxidation process (AOP)**	**Analysis performed**	**Results**	**Reference**
Dimethyl sulphur oxide (widely used in the manufacture of electronics, polymers, dyes, membranes, etc.)	Activated-Sludge biosystem	Fenton process	TOC, COD, BOD	BOD5/COD ratio increased from 0.035 to 0.87. 90% removal of TOC from activated sludge system. Integrated system was not efficient	(Vaiano et al., 2016)
Reverse osmosis of brine from water reclamation facilities	Biological activated carbon system	Ozonation	TOC, BOD5, colour, anions and cations concentration (ionic chromatography)	Combined system achieved 3 times higher TOC removal compared to using the biological activated carbon process alone	(Yan et al., 2010)

(Wastewater) Pollutants degraded	Biological treatment	Advance oxidation process (AOP)	Analysis performed	Results	Reference
Trihalomethanes (THMs) precursor	Biological granular activated carbon filtration	Ozonation	TOC, turbidity, alkalinity, iodine, GC	Integration process was superior to granular activated carbon system to THMs precursor removal	(Lee et al., 2009)
Raw Paper Mill wastewater (bleaching process)	Activated sludge biotreatment	Ultrasonic process	COD, TOC, Vibrio fischeri toxicity test, BOD5/COD	The combined treatment was inefficient for concentrated basic paper mill wastewater. The acidification of the solution accelerated oxidation and mineralization. Biodegradability rate improved at the end of the combined process	(Xu et al., 2020)
Paper Mill wastewater (pulp mill alkaline bleach plant effluent)	Batch aerobic biological system	Ozonation	COD, TOC, BOD5 and molecular weight distribution	20% organic compounds removal in ozonation pre-treatment. 30% TOC removal during biological process	(Bijan and Mohseni, 2005)
Paper Mill wastewater (Kraft pulp mills)	Activated sludge biotreatment	Ozonation (membrane pre-treatment)	COD, BOD5, total carbon, colour and ozone	Biodegradability of the wastewater during the ozone oxidation increased significantly	(Bijan and Mohseni, 2005)
Disinfection by-products (trihalomethanes and halo acetic acids)	Biological activated carbon treatment	UV-H_2O_2	Disinfection by-products concentrations TOC, absorbance at 254 nm (UV254)	The combined treatment showed reductions of 43%, 52% and 59% for disinfection by-products, TOC and UV254, respectively	(Toor and Mohseni, 2007)
Substituted phenols	Enzyme treatment	Sonolysis	Contaminant concentration (HPLC)	Combined method more efficient for phenol and its halogenated derivatives	(Entezari and Pétrier, 2003)
Real industrial wastewater containing AMB	Fixed bed biological reactor	Fe (III)-photo-assisted process (suntest simulator/CPC reactor)	TOC, COD, AMBI concentration (HPLC), Zahn-Wellens test	70% of AMBI eliminated 90% of TOC removal in the combined system	(Sarria et al., 2003)
Chlorinated organic substances (4-chlorophenol)	Activated sludge biotreatment	Fenton process	COD, BOD	Biodegradation rate enhanced two-fold by the application of the combined system	(Kamali et al., 2021)

2.3 The novel integrated system components

An integrated system has a combination of two or more treatment techniques such as biological, chemical, and physical processes. Basically, this configuration can be classed into four (4) categories, i.e. (i) physical-biological hybrid system, (ii) physical-chemical hybrid system, (iii) chemical-biological hybrid system and finally (iv) physical-chemical-biological hybrid system (Adetunji and Olaniran, 2021; Ratna et al., 2021). As shown in Table 1, AOPs can be integrated with AD systems for remediation of various wastewater. This suggests that the development of an integrated treatment process is essential to provide a solution to wastewater environmentally challenged problems. Notwithstanding, the importance of this combination will also provide energy savings, resource recovery and increased overall efficiency of the system. Therefore, to provide sustainable energy and water supply for socioeconomic growth and activities warrants cost-effective technologies (De Clercq et al., 2017; Popp et al., 2014). Herein, this project explored the option of an integrated AD-AOP magnetised system (Figure 2) for the valorisation of wastewater towards bioeconomy.

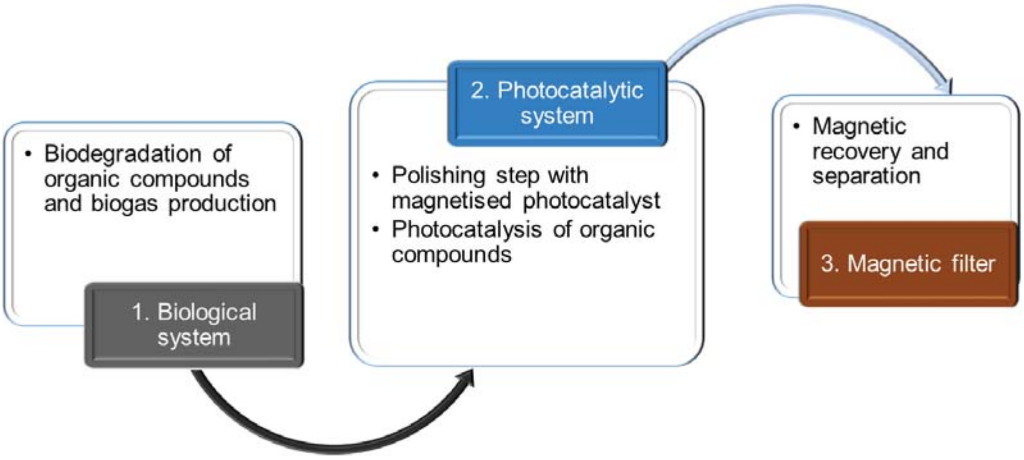

Figure 2: Proposed integrated AD-AOP magnetised system

2.3.1 Anaerobic digestion (AD)

With the recent South African energy-driven economy, meeting the country's high energy demand warrants upgrading of WWTP capacities to balance their energy throughput and utilization (Lin and Sai, 2021; Russo and Von Blottnitz, 2017). In essence, the paradigm shift of WWTPs into the bioeconomy involves the use of AD to degrade complex organic matter into biogas (CH_4, CO_2) (Rojo et al., 2021). Notwithstanding, the AD process has proven to be advantageous in terms of adding value to wastewater as a bioenergy resource (Durán et al., 2021; Russo and Von Blottnitz, 2017; Zhao et al., 2021a). However, the AD process is mainly governed by the oxidation state of the organic waste digested, environmental conditions, and the AD reactor configurations (Apollo et al., 2013; Rojo et al., 2021; Zhao et al., 2021a). In fact, the biological processes are considered to be cost effective in terms of operational cost, however, initial investment cost maybe higher depending on the type and configuration of the reactor (Paździor et al., 2019). Figure 3 shows various types of AD reactor configurations and operating factors are depicted in Figure 4. Meanwhile, the AD mechanism involving hydrolysis, acidogenesis, acetogenesis, and methanogenesis to produce methane potential is kinectically very slow and requires long retention times (Ajay et al., 2020; Apollo et al., 2013; Rojo et al., 2021). For instance, methane-producing bacteria (hydrogenotrophic methanogenesis) activities (2.1) are faster than acetotrophic methanogens, which use acetate routes (2.2) to produce methane (CH_4).

In addressing these setbacks, this study proposed an AD process coupled with photocatalytic technology coupled with magnetic separation as a wastewater abatement technology for bioenergy production with econoically and environmentally sustainable options.

$$4H_2 + CO_2 \rightarrow CH_4 + 2H_2O \quad (2.1)$$

$$CH_3COOH \rightarrow CH_4 + CO_2 \quad (2.2)$$

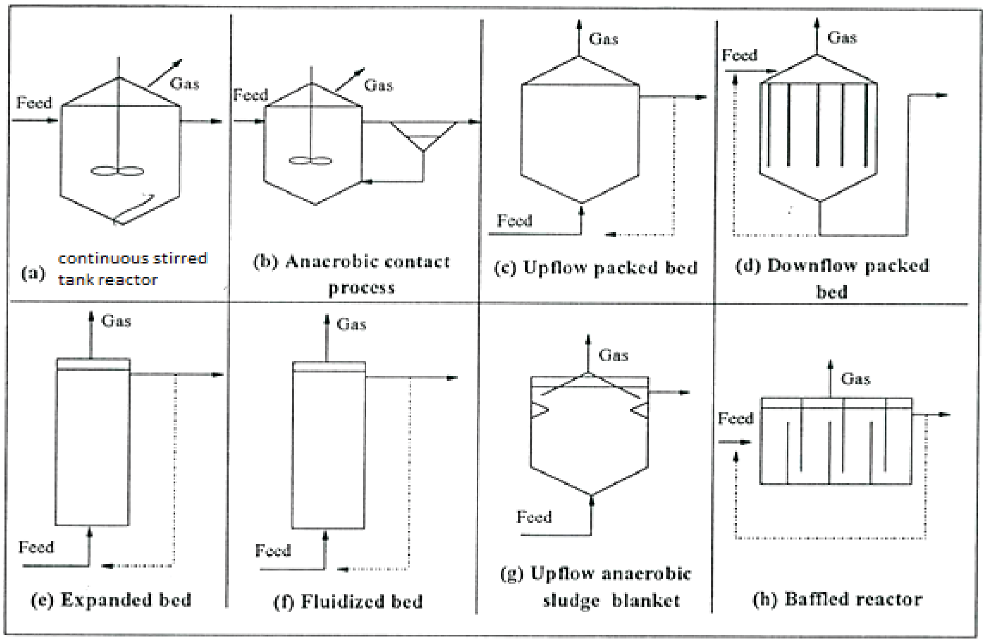

Figure 3: Anaerobic digester configurations (Appels et al., 2008)

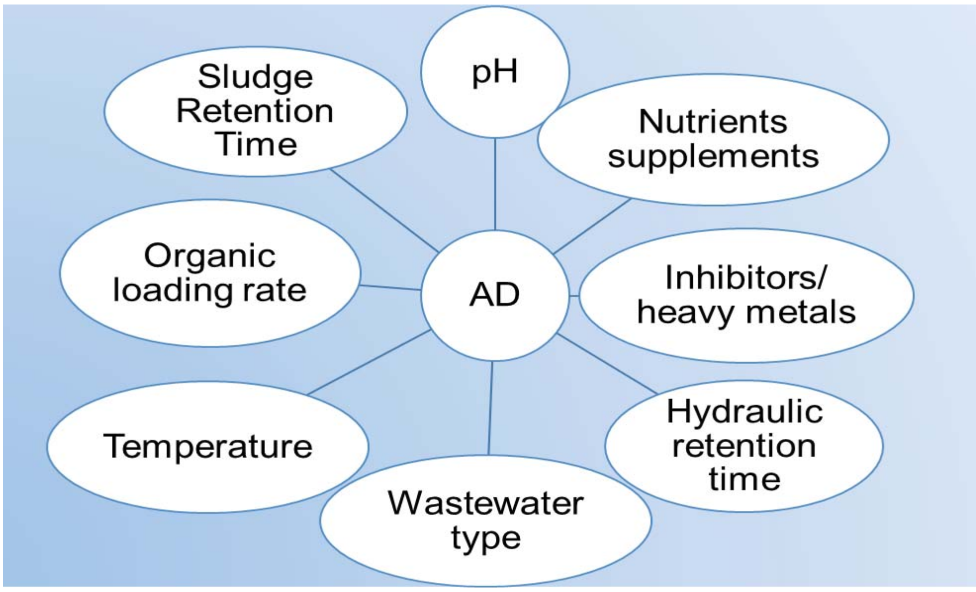

Figure 4: Operating parameters that governs anaerobic digestion processes

2.3.2 Advanced oxidation processes (AOPs)

Advanced oxidation processes (AOPs) can be classified into three groups; chemical oxidation (O_3, O_3/H_2O_2), photochemical oxidation (Ultraviolet-UV/O_3, UV/H_2O_2) and heterogeneous photocatalysis (UV/TiO_2) (Bethi et al., 2016; Kanakaraju et al., 2018; Oller et al., 2011). Among them, the ability to generate effective reactive hydroxyl radicals with photon energy, without the need of additional chemicals makes the photocatalysis process very attractive. AOPs are used for pre- and post-treatment of wastewater via the generation of strong oxidants such as hydroxyl radicals (•OH) for the oxidation of organic compounds (Mohapatra & Kirpalani, 2019; Tetteh et al., 2020). In photocatalytic oxidation, a semiconductor photocatalyst is illuminated by light of a suitable wavelength to generate hydroxyl radicals that can initiate a chain of redox reactions to degrade organic pollutants (Figure 5). The most effective photocatalyst for widespread environmental application is titanium dioxide (TiO_2). In fact, pH, catalyst loading, amount of oxygen, contaminant loading, light intensity and temperature are among the factors that can influence AOP performance and hence requires optimisation (Mecha et al., 2016).

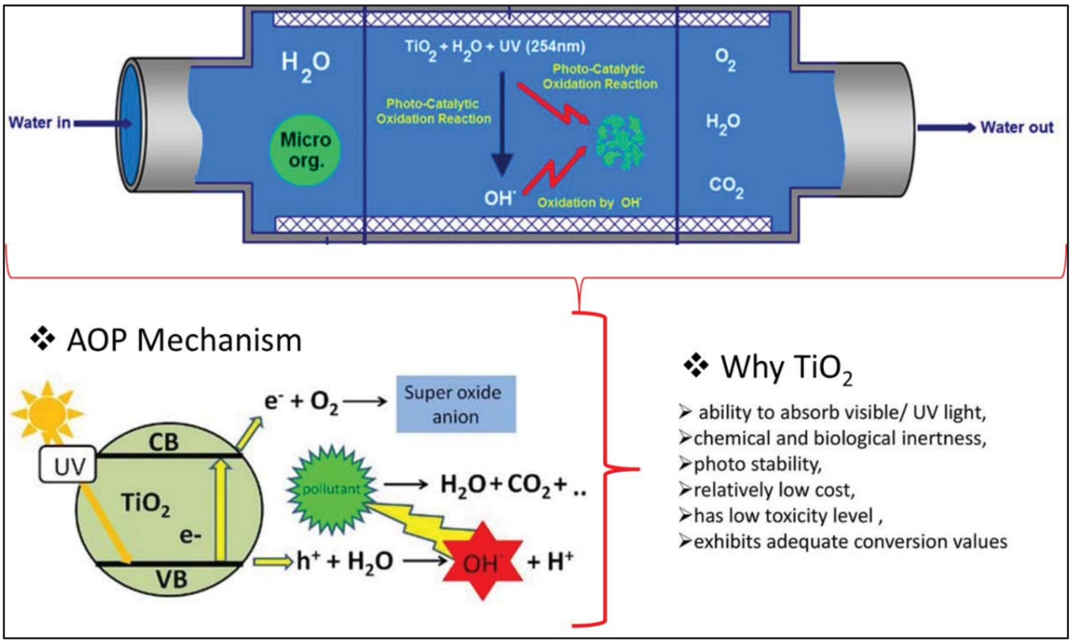

Figure 5: Schematic diagram of the advanced oxidation process (AOP) mechanism

The photocatalytic mechanism as shown in Figure 5Figure 5 involves the breaking down of the complex organic compounds into carbon dioxide (CO_2), water (H_2O) and other intermediate compounds. In spite of the great advantages of the TiO_2 photocatalysis, its large scale application is very limited due to high process costs resulting from the use of reagents/catalysts and light energy source (electricity) (Kanakaraju et al., 2018; Lee & Park, 2013). However, such limitations can be minimized with better equipment designs that promotes more efficient mass transfer and recovery and reuse of the photocatalysts (Kweinor Tetteh and Rathilal, 2021; Watson et al., 2002). In terms of the TiO_2 photochemistry (Figure 5), when the photon energy (hv) becomes equal or greater than the bandgap, the excited electrons (e^-) in the valance band (VB) then shift towards the empty conduction band (CB). The outcome is a positive region formation in the VB holes (h^+) and as such free electrons (e-) in the CB (2.3) (Dong et al., 2015; Suzuki et al., 2015).

$$TiO_2 \xrightarrow{hv} TiO_2 + e^-(CB) + h^+(VB) \quad (2.3)$$

The catalyst's holes react (2.4) with hydroxyl ions (OH-), absorbing water and forming hydroxyl free radicals (•OH) (Dong et al., 2015; Mecha et al., 2016; Suzuki et al., 2015).

$$TiO_2(h^+) + OH^- \rightarrow TiO_2 + \bullet\, OH \quad (2.4)$$

The CB electron reduces oxygen to the superoxide ion: $O_2^{\bullet -}$ (2.5). This reaction prevents the e-/h+ from recombining; this happens when other electron acceptors such as pollutants are absent.

$$O_2 + e^- \rightarrow O_2^{\bullet -} \quad (2.5)$$

H_2O_2 is produced by the further reduction of $O_2^{\bullet -}$ (2.6)

$$O_2^{\bullet -} + e^- 2H^+ \rightarrow H_2O_2 \quad (2.6)$$

The superoxide ion which is in its protonated form subsequently compete to produce hydrogen peroxide or a peroxide anion (2.7-2.9)

$$O_2^{\bullet -} + H^+ \rightarrow HO_2^{\bullet} \quad (2.7)$$

$$O_2^{\bullet -} 4HO_2^{\bullet} \rightarrow 2 \bullet OH + 3O_2 + H_2O_2 \quad (2.8)$$

$$2HO_2^{\bullet} \rightarrow O_2 + H_2O_2 \quad (2.9)$$

The addition of H_2O_2 is said to increase the photodegradation rate under certain conditions either through the formation of •OH radicals (2.10) or the reduction of H_2O_2 by the CB e^- (2.11).

$$O_2^{\bullet -} + H_2O_2 \rightarrow \bullet\, \mathrm{OH} + OH^- + O_2 \quad (2.10)$$

$$H_2O_2 + e^- \rightarrow \bullet\, OH + OH^- \quad (2.11)$$

The recombination of the •OH could lead to the formation of hydrogen peroxide (2.12).

$$\bullet\, OH + \bullet\, OH \rightarrow H_2O_2 \quad (2.12)$$

2.3.3 Magnetic photocatalysts (MPCs)

Titanium dioxide (TiO_2) has been utilized as a photocatalyst since the 1970s because of its stable semiconductor properties for wastewater treatment (Guo et al., 2019; Riaz and Park, 2020). As shown in Figure 6, TiO_2 polymorphs have different properties as rutile (stable at a high temperature), brookite (usually found in minerals with an orthorhombic crystal structure), and anatase (stable at low temperature). Unfortunately, the use of conventional TiO_2 nanoparticles is difficult to separate and recover after photocatalytic activity and inactive in solar energy utilization for large-scale production (Abdulhameed et al., 2019; Riaz and Park, 2020; Thakre et al., 2021; Zhao et al., 2021b). Thus, slurry-type reactors require a post-seperation process with additional chemical treatment, which are still difficult to recover fine photocalyt particles from the treated water. This is a major problem in water and wastewater treatment settings as it comes with extra costs and treatment efficieny, thereby limiting commercial usage of the TiO_2. To overcome this obstacle, this work used co-precipitation to produce MPCs with high surface area, physiochemical stability, and magnetic separation ability (Riaz and Park, 2020; Xu et al., 2021). Based on *in situ* generation of highly reactive species, the TiO_2 photocatalysis can completely mineralize organic contaminants into non-toxic and biodegradable intermediate compounds (Mecha et al., 2016).

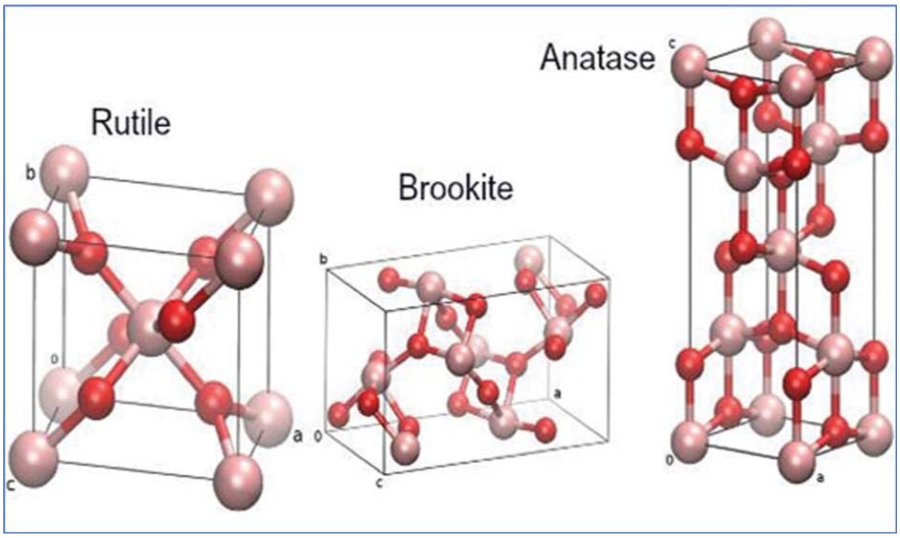

Figure 6: Crystal structure of TiO_2 rutile, brookite and anatase; adapted from Kim et al. (1996)

2.4 Overview of synthesising techniques

This section highlights an overview of techniques commonly used for developing a stable magnetic photocatalyst. This makes for easy recovery and separation by an external magnetic field and also more reliable for the reusability of the photocatalysts. Table 2 presents a summary of some of the techniques employed for preparing magnetic nanoparticles (MNPs). The synthesis of the MNPs plays an important role in tailoring the particle morphology, composition and surface properties (Sharma et al., 2016). Mohammed et al. (2017) grouped these methods into physical, wet chemical and microbial methods. The wet chemical method includes chemical co-precipitation reactions in constrained environments, hydrothermal, sol-gel reactions, polyol methods, flow injection syntheses, electrochemical and aerosol/vapour methods (Lai et al., 2018). Others are sonolysis, thermal decomposition, hydrolytic and non-hydrolytic wet chemistry methods, liquid phase, micro-emulsion, and laser evaporation synthesis (Liu et al., 2020).

Table 2: Synthesis techniques and their properties, adapted from Kiser et al. (2009) and Lu et al. (2007)

Method of synthesis	**Co-operation**	**Microemulsion**	**Thermal decomposition**	**Hydrothermal synthesis**
Techniques	Very simple, ambient condition	Simple	Simple, inert atmosphere	Simple, high pressure
Reaction period	Hours	Hours	Hours-days	Hours
Component	Water	Organic compound, water	Organic compound	Water-ethanol
Reaction temperature (°C)	20-90	20-50	100-320	220
Size distribution	Relatively narrow	Relatively narrow	Very narrow	Very narrow
Shape control	Good	Good	Very good	Very good
Yield	High	Low	High	Medium

2.4.1 Magnetised nanoparticles (MNPs) and magnetic separation

The interaction between negatively and positively charged nanoparticles can be heightened by augmenting their magnetic and particle valence charges (Elhambakhsh et al., 2020). Herein, employing MNPs in solid-liquid separation technologies can improve the particle settling efficiency as the interactions get stronger and agglomerate. Also, the MNPs can be recovered by an external magnetic field, recycled, and regenerated for use in other applications while retaining greater treatability performance (Álvarez et al., 2010; Gao and Zeng, 2003; Malato et al., 2009). There are no risks associated with using a magnetic field to improve a system. This technique can save money by using permanent magnets as an aid because they are only purchased once at the beginning of installation. This makes the use of magnetic fields in water and wastewater advantageous for being regarded as a sustainable and green technology. Table 3 presents a survey of applications of MNPs in the water and wastewater settings as well as that of the current studies.

Table 3: Overview of magnetic nanomaterials and their applications

Nanoparticles	**Synthesis method**	**Application**	**Reference**
Magnetic chitosan-GO	Hummer-Offerman method	Heavy metal removal (chromium)	(Debnath et al., 2014; Kyzas et al., 2014)
Chitosan-Silica	Sol-gel	Pharmacological, biomedical, and waste treatment products	(Ayers and Hunt, 2001)
$NiFe_2O_4$ coated on reduced GO	Hydrothermal	Supercapacitors for energy storage and application	(Askari and Salarizadeh, 2020; Gao et al., 2020)
Magnetic TiO_2	Ultrasonic assisted sol-gel	Photodegradation of contaminant in water	(Álvarez et al., 2010; Gao and Zeng, 2003; Malato et al., 2009)
Magnetite (Fe_3O_4)	Co-precipitation	Absorption of CO_2	(Elhambakhsh et al. 2020)
Nickel magnetite photocatalyst ($NiFe_2O_4$ TiO_2)	Co-precipitation and sol-gel	Photocatalyst for humic acid degradation	(Khodadadi et al., 2020)
TiO_2 – PSF membrane	Hydrothermal	Removal of NaCl	(Amini et al., 2016)
Fe/Al-TiO_2, Fe/Cu-TiO_2, Fe/Ch-TiO_2, Fe_3O_4 and Fe-TiO_2	Coprecipitation	Biogas and methane enhancement, wastewater treatment	This study

Chapter 3: Synthesis, characterization, and application of MPCs

This section presents the co-precipitation technique of synthesizing the novel magnetized photocatalysts (MPCs) with beneficiation of recoverability for reuse in industrial wastewater treatment. The materials and assay protocol used together with the analytical techniques to attest to the success of the engineered MPCs are discussed. In essence, a series of feasibility studies and engineering works were explored on MPCs (Fe/Al-TiO_2, Fe/Cu-TiO_2, TiO_2, Fe/Ch-TiO_2, Fe_3O_4 and Fe-TiO_2), and other MNPs as depicted in Table 3. It was elucidated that the tailored MPCs have great potential to improve wastewater and biogas quality, and also easily recovered with an external magnetic field. Further discussions on technological evaluation and application of MPCs by using the integrated system are presented in Chapter 4.

3.1 Co-precipitation synthesis

The MPCs were prepared using the co-precipitation assay adapted from El Ghandoor et al. (2012). The binary and ternary nanocomposite preparation, a precursor of bimetallic magnetite (Fe_3O_4) was prepared as a precursor in a 1:1 volume ratio (0.5 L/0.5 L) of Fe^{3+} and Fe^{2+} stock solutions. The same procedure was repeated for the binary and ternary MPCs, respectively using a volume ratio of 3:2:1 (Fe^{3+}/Fe^{2+}/TiO_2) and 3:2:1:1 for Fe^{3+}/Fe^{2+}/TiO_2/(Al or Ch). Table 4 shows the techniques employed for the characterisation of the MPCs.

Table 4: Characterisation techniques and their purposes

Method	Purpose	Location
X-ray diffraction (XRD) (Bruker AXS, D8 Advance, Germany) coupled with PANalytical software (Empyrean, PRO MPD, Netherlands)	Phase identification	iThemba LABS, Materials Research Department, South Africa.
Fourier Transform Infrared (FTIR) spectrometer (Shimadzu FTIR 8400)	Predictions of the band lengths, functional group identifications of organics and inorganics	Department of Chemical Engineering, Durban University of Technology, SA
Scanning electron microscopy and energy dispersive X-ray (Nova NanoSEM coupled with EDT and TLD detector)	Surface morphology and elemental quantification and identification	The Electron Microscope Unit of University of Cape Town
Brunauer-Emmett-Teller (BET) Micrometric analyser (TriStar II Plus, GA, USA)	Surface area, pore size and pore volume	Department of Chemical Engineering, Durban University of Technology, SA

3.2 Surface area, pore size, and pore volume of MPCs

The BET surface area, pore-volume, and mesopore diameter distribution estimated by the Barret-Joyner-Halenda (BJH) are depicted in Table 5. It is eluded that the MPCs BJH pore size increased the surface area, as the Fe-TiO_2 was found to have the highest surface area (62.73 m^2/g). The success of the TiO_2 transformation and surface area modified with the Fe_3O_4 affirms other reported studies (Álvarez et al., 2010; Askari and Salarizadeh, 2020; Debnath et al., 2014; Kamal et al., 2017; Rezlescu et al., 2014; Saiz et al., 2014). Fe/Cu-TiO_2, due to its low surface area (28.85 m^2/g) in this case, was not considered for the integrated system evaluation.

Table: 5 BET surface morphology

Name	Catalyst type	BET Surface area (m^2/g)	Pore volume (cm^3/g)	BJH pore size (nm)
Magnetite	Fe_3O_4	27.6	0.008	1.484
Titanium dioxide	TiO_2	25.7	0.11	0.16
Magnetite/TiO_2	Fe-TiO_2	62.73	0.017	1.337
Magnetite/Chitosan/TiO_2	Fe/Ch-TiO_2	54.85	0.004	0.286
Magnetite/Chitosan/TiO_2	Fe/Al-TiO_2	30.02	0.009	1.144
Magnetite/Chitosan/TiO_2	Fe/Cu-TiO_2	28.85	0.008	1.453

3.3 Morphology and elemental composition of the MPCs

The morphology and elemental composition of the MPCs were defined by the scanning electron microscopy and energy dispersive X-ray detector (SEM/EDX) analysis. The SEM/EDX images affirm the uniform distribution of the TiO_2 and Fe over the MPCs of the (a) Fe/Al-TiO_2, (b) Fe/Cu-TiO_2, (c) TiO_2, (d) Fe/Ch-TiO_2, (e) Fe_3O_4 and (f) Fe-TiO_2 with the elemental compositions shown in Table 6 .

Table 6: Elemental compositions of MPCs

Elements	C (%)	O (%)	Al (%)	S (%)	Na (%)	Cu (%)	Fe (%)	Ti (%)
Fe_3O_4	27.59	44.17					28.23	
TiO_2		57.83						42.17
Fe-TiO_2	7.67	45.48					30.04	16.81
Fe/Ch-TiO_2	8.1	55.53			13.15		6.94	22.28
Fe/Al-TiO_2	22.83	55.12	2.57	5.2			6.34	7.93
Fe/Cu-TiO_2	19.2	51.43			15.49	0.48	1.95	11.45

From Table 6, the inclusion of Fe in the MPCs (Fe/Al-TiO_2, Fe/Cu-TiO_2, Fe/Ch-TiO_2, Fe-TiO_2) expedited their paramagnetic phase transformation and charge reaction (3.1-3.2). This valance change might also be due to the heating, whereby the Fe reduction promoted the oxidation reaction (3.3). Similarly, the cationic dopants (Al/Cu) have many valences and hence the possibility for reduction-oxidation processes (3.4). This increased oxygen vacancies (promoted phase change via lattice relaxation) and/or Ti^{3+} bridging formation (inhibition of the phase transformation through lattice constraint). The generation of oxygen vacancies by the reduction of dopant Fe/Al in the TiO_2 lattice may assist the anatase to rutile phase transition (14 and 16). Also using the divalent Cu^{2+} has the tendency of producing tenorite (CuO) or cuprite (Cu_2O) photocatalysts (β-Cu/TiO_2), with some complexity. Likewise, the use of chitosan with Na^+ dominacy (Table 6) also produces sodium oxide (Na_2O) photocatalysts (γ-Na-TiO_2).

$$FeSO_4 \cdot 7H_2O + 2FeCl_3 \cdot 6H_2O + 8NaOH \rightarrow Fe_3O_4 + 6NaCl + 23H_2O + Na_2SO_4 \tag{3.1}$$

$$Fe^{3+} + Ti^{4+} + 2O^{2-} \rightarrow (Fe^{2+} + O^{2-} + \Delta_a) + Ti^{3+} + \frac{1}{2}O_2 \tag{3.2}$$

$$2Fe^{3+} + O^{2-} \rightarrow 2Fe^{2+} + \Delta_a + \frac{1}{2}O_2 \tag{3.3}$$

$$Al^{3+} + Ti^{4+} + 2O^{2-} \rightarrow \left(Al^{3+} + \frac{3}{2}O^{2-} + \frac{1}{2}\Delta_a\right) + Ti^{3+} + \frac{1}{4}O_2 \quad (3.4)$$

Where Δ_a denotes an anion vacancy.

3.4 Crystal structures of the MPCs

The X-ray diffraction (XRD) was used to determine the MPC crystallinity and polymorphic phases, where the MPC crystal diffractograms corresponding to their peaks were confirmed by the JCPDS (Joint Committee on Powder Diffraction Standards) files presented in Table 7. The MPCs' strong crystalline structure (227) showed the magnetite (Fe_3O_4) in all modified MPCs. TiO_2 embedded in the MPCs exhibited anatase crystalline structures with peaks corresponding to (141). Additionally, the forms of iron oxides, classically ferrimagnetite, ferromagnetite, maghemite, mikasite, magnesioferrite, thermonatrite, sylvite and so on were also identified (Table 7). Among them, magnetite and maghemite are reported to be very promising with good biocompatibility and superparamagnetic potential (El Ghandoor et al., 2012; Kobwittaya and Sirivithayapakorn, 2014).

Table 7: Physio-chemical properties of the MPCs obtained from the XRD JCPDS file

2θ (degree)	Miller indices (hkl) plane	dhkl (nm)	Crystal structure	Nanostructure	JCPDS pattern
24.865	(62)	3.549	Orthohombic	β-$FeSO_4$	00-033-0682
21.398	(14)	3.202	Monoclinic	ferrimagnetite	00-070-2091
48.491	(12)	2.106	Monoclinic	Clinoptilolite	01-071-1425
65.976	(227)	5.42	Face-centered cubic	Cupper iron oxide	01-077-0010
84.582	(148)	2.856	Rhombohedral	Aluminium sulfate	01-077-0385
29.406	(167)	2.711	Rhombohedral	Calcite	00-005-0586
51.44	(44)	2.162	Base-centered orthohombic	Sodium nitrate	01-075-2073
27.335	(225)	2.163	Face-centered cubic	Halite	00-005-0628
41.806	(150)	1.712	Hexagonal	Antarcticite	00-026-1053
35.423	(227)	5.197	Face-centered cubic	Magnetite (Fe_3O_4)	00-019-0629
25.281	(141)	3.893	Body-centered tetragonal	Anatase (TiO_2)	00-021-1272
33.153	(167)	5.27	Rhombohedral	Hematite (α-Fe_2O_3)	00-033-0664
35.631	(213)	4.858	Cubic	Maghemite (γ-Fe_2O_3)	00-039-1346

3.5 Summary

The co-precipitation technique was used to synthesize the MPCs and by exploring their potential for wastewater treatment was found feasible. Analytically, characterization of the MPCs via SEM/EDX, XRD, FTIR and BET techniques revealed successful modification of the TiO_2 in its binary (Fe-TiO_2) and ternary (Fe/Al-TiO_2 and Fe/Cu-TiO_2, Fe/Ch-TiO_2) forms. In essence, the distribution of the Fe_3O_4 on the TiO_2 surface was affirmed with the SEM/EDX, whereas the XRD and FTIR spectra respectively revealed the crystalline structure and functional monomers of the MPCs. Among the MPCs, the BET showed that Fe-TiO_2 had the highest surface area (62.73 m^2/g) with a pore volume of 0.017 cm^3/g and pore size of 1.337 nm. Therefore, to improve the MPCs, Fe-TiO_2 was found to be more competitive than its commercialised counterparts (TiO_2) so was considered for the subsequent investigations.

Chapter 4: An integrated AD-AOP magnetised system: design and evaluation

This section presents design, monitoring, and evaluation of the lab-scale integrated anaerobic-photo-catalytic-magnetic system for municipality wastewater treatment.

4.1 Design and fabrication of the AD-AOP magnetised system

(i) Design factors:

The AD-AOP magnetized system was designed based on operational factors that affect the production of biogas and photocatalysis processes. Some of the operational factors considered were the temperature, pH, agitation, type of wastewater, water quality, catalyst type as well as the light source (McCabe et al., 2018; Brooms et al., 2020). Other factors such as maintenance, durability, corrosion, toxicity, separation, and recoverability of the magnetised photocatalyst were also considered for the selection of the materials used for the fabrication. The dimensions of the various components were chosen to minimize the size, based on availability of effluent load required and operational cost while not jeopardizing the system efficiency.

(ii) Components required:

Aside the biodigesters, a photoreactor (Figure 7a) and magnetic filter (Figure 7b), biogas analyser, flexible silicon tubes, flexible Polyvinyl chloride (PVC), plugs, multi-plug, electrical wire, pliers, sealant, valves, and fittings were among the additional resources and machinery used.

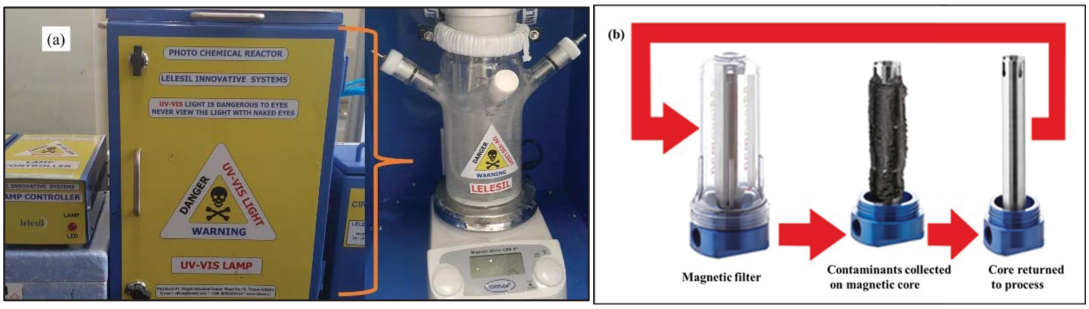

Figure 7: Cross section view of (a) photocatalytic reactor setup and (b) magnetic filter

(iii) Fabricated AD-AOP system:

The lab scale integrated system, involving an anaerobic reactor (AD), buffer reactor (AN), photocatalytic reactor (AOP) and magnetic filter (MS) components assembled for the treatment of the eThekwini Municipality wastewater is presented in Figure 8.

(iv) Installation and commission.

After the installation of the system components, the integrated AD-AOP magnetised system (Figure 8) was commissioned. The pumps were calibrated to know their respective flowrates.

The low-high pump speed of 10-80% corresponded to average flowrates of 20-200 mL/min for P1 and P3, whereas P2 recorded 23-175 mL/min. To maintain the temperature of the AD process, the hotplate was regulated to maintain mesophilic temperature (30-45°C), whereas the hotplate 2 was adjusted to an intermittent slow mixing rate of 15 rpm. The AOP reactor was also regulated within 15-45 rpm. To ascertain the performance of the system, all conditions were kept constant, while different types of MPCs (Fe-TiO_2, Fe/Al-TiO_2, Fe/Ch-TiO_2, Fe_3O_4 and TiO_2) were investigated.

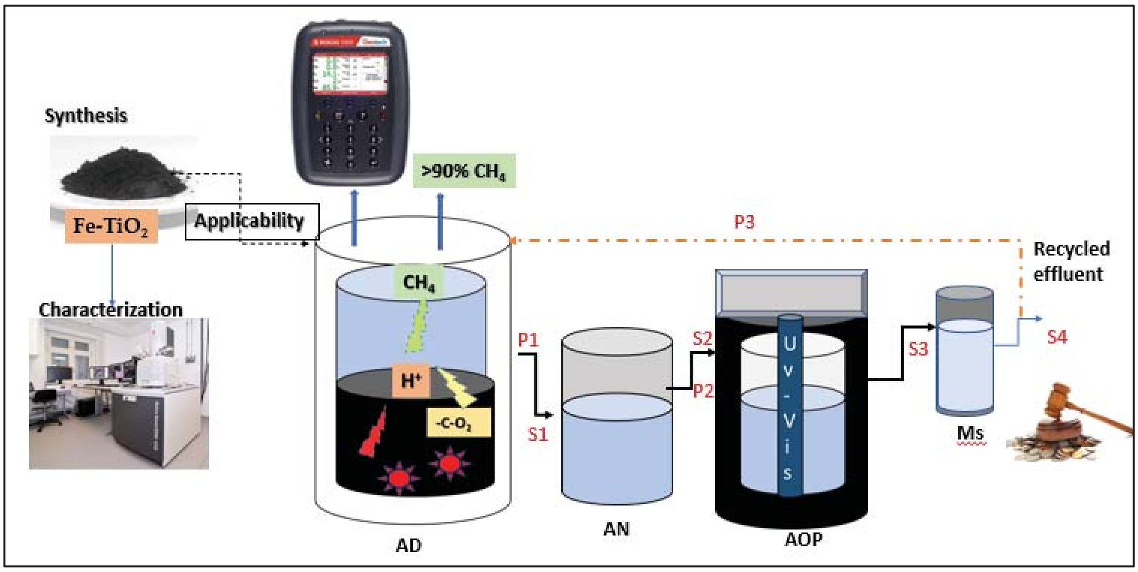

Figure 8: Graphical representation of the integrated system in operation; AD-anaerobic digestion; AN-buffer system; AOP-advanced oxidation process; Ms-magnetic field, P1-P3-pumps; S1-S4-sample points

(v) Operation of the AD-AOP

The experiment was set up as a semi-batch continuous process with the AD-AOP magnetised system assembled as shown in Figure 8. Wastewater sample used as a feedstock was obtained from a local wastewater treatment plant in the KwaZulu-Natal province, South Africa. A good operational condition was established via a checklist. Samples were taken daily from each unit sample point, i.e. AD-S1, AN-S2, AOP-S3 and MS-S4, for characterisation. The system biogas production was monitored daily via download dis-placement measurement and its corresponding water quality was then characterised. A Portable Biogas Analyser (Geotech Biogas 5000, UK) was used to characterise the biogas composition weekly.

4.2 Evaluating the MPCs

The impact of the MPCs was assessed by the integrated system with respect to biogas and methane production, photochemistry of the wastewater (COD removal), as well as the sequential removal of toxicological trace elements by the magnetic field employed.

4.2.1 Biogas production and methane content

Figure 9 shows the biogas produced with and without MPC additives, whose assay respectively revealed biogas production and methane content trend of No-charge < TiO_2 < Fe/Al-TiO_2 < Fe/Ch-TiO_2 < Fe-TiO_2. Generally, the degree of degradation of high organic compounds (in terms of COD removal) is expressed as a function of biogas produced with 50-65% methane content (Reza et al., 2014; Hülsemann et al., 2020). Therefore, in comparing the control (No-

Charge) to that of MPC impact on the methane enhancement in the biogas produced (Figure 9), more than 75% CH_4 was achieved.

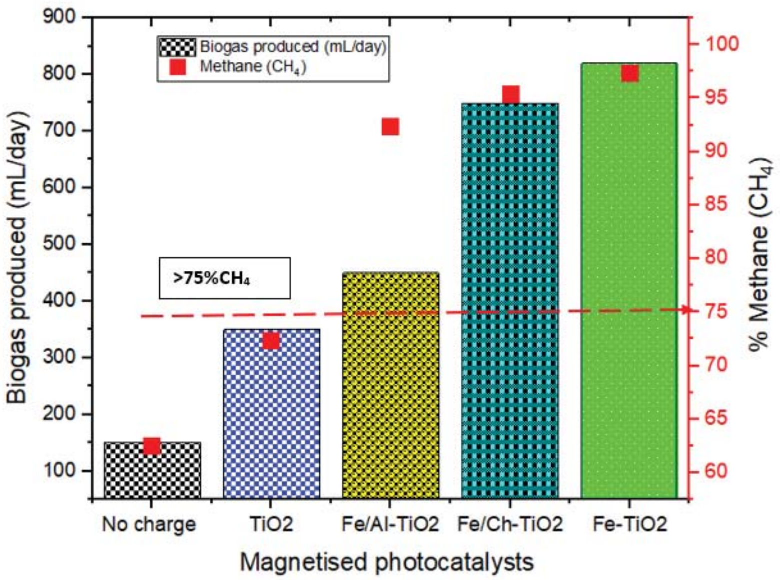

Figure 9: Effect of magnetised photocatalysts on biogas production and methane yield using an integrated AD-AOP magnetised system

4.2.2 Effects of MPCs on COD removal

Also, using No-catalyst charge as the basis of the system, the performance of TiO_2 photocatalyst was compared to three engineered magnetised photocatalysts herein named as Fe-TiO_2, Fe/Ch-TiO_2, and Fe/Al-TiO_2. As shown in Figure 10, Fe-TiO_2 was found as the most superlative MPC, hence its effluent was furthermore characterised to account for the trace elements and their removal (Table).

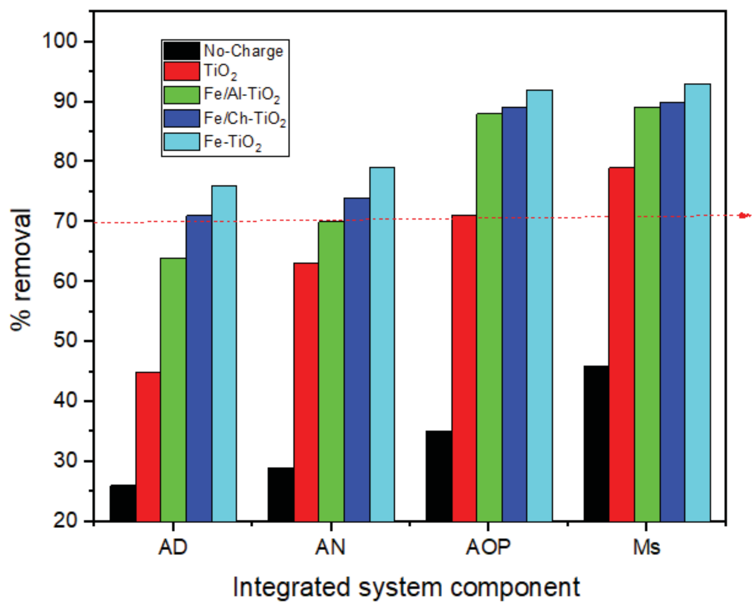

Figure 10: Effects of MPCs on COD removal using the integrated system component units; AD-anaerobic digestion; AN-buffer system; AOP-advanced oxidation process; Ms-Magnetic filter system

4.2.3 Toxicological analysis of the trace element

In this context, the effluent with the Fe-TiO_2 additives was characterised to account for the trace elements. Table 8 shows the reduction and deficiency of 27 trace elements detected in the wastewater via the integrated AD-AOP magnetised system. Evidently, the presence of the magnetic filter (MS) facilitated the reduction of most of the trace elements (e.g. Fe, Ti) after the AOP system. Notwithstanding the toxicological testing of the engineered nanomaterials in water and wastewater settings is at its early stages, tracking of the trace elements in the integrated system component was found valuable.

Table 8: Trace elemental composition and deficiency by each unit of the integrated system

Number	Trace element	Feed (mg/L)	AD (mg/L)	AN (mg/L)	AOP (mg/L)	MS (mg/L)
1	Si	N/A	N/A	N/A	N/A	N/A
2	V	2.775	0.869	0.994	0.964	0.952
3	Zn	0.42	0.107	0.088	0.096	0.11
4	Ag	4.38	2.01	0.827	0.365	0.199
5	Al	32.545	15.805	4.835	5.802	1.779
6	As	0.025	0.031	0.02	0.001	0.005
7	Ba	0.75	0.167	0.212	0.289	0.257
8	Be	0.04	0.022	0.024	0.023	0.026
9	Ca	437.99	65.58	62.39	66.203	58.182
10	Cd	0.075	0.006	0.004	0.006	0
11	Co	0.03	0.003	0.04	0.007	0.038
12	Cr	1.445	0.179	0.122	0.306	0.129
13	Cu	1.32	0.371	0.199	0.147	0.11
14	Fe	0.038	0.223	0.209	0.068	0.025
15	K	463.985	154.606	175.714	171.189	177.426
16	Mg	84.06	15.248	15.048	15.979	15.784
17	Mn	0.75	0.09	0.112	0.084	0.071
18	Mo	N/A	N/A	N/A	N/A	N/A
19	Na	741.78	111.346	86.068	97.433	103.963
20	Ni	5.565	0.364	0.701	0.999	1.989
21	Pb	0.145	0.013	0.059	0.052	0.004
22	Sb	0.015	0.016	0.005	0.035	0.031
23	Se	0.22	0.02	0.016	0.005	0.038
24	Sn	0.1	0.003	0.003	0.006	0.015
25	Sr	N/A	N/A	N/A	N/A	N/A
26	Ti	0.77	0.552	0.533	0.274	0.119
27	Tl	0.12	0.029	0.006	0.014	0.007

4.3 Summary on MPCs evaluation

The impact of magnetised photocatalyst ($Fe\text{-}TiO_2$ > $Fe/Ch\text{-}TiO_2$ > $Fe/Al\text{-}TiO_2$) tailored via the co-precipitation technique was employed and compared to that of unmodified TiO_2 photocatalyst. The degree of degradation of the high organic strength wastewater (COD) and reduction of 27 trace elements by the integrated system was highlighted. Moreso, the presence of $Fe\text{-}TiO_2$ in the AD and AOP processes favoured the oxidization potentials of the organics into simple compounds. Some of the benefits of the $Fe\text{-}TiO_2$ included

- It had the capacity to buffer the oxidation reduction potential in the system,
- It facilitated the enzymatic activities, like Fe-S clusters,
- Its reaction with the sulphide and hydrogen molecules resulted in an increase of biogas methane potential (>90% CH_4) yield, which suppressed its hydrogen sulphide and CO_2 levels.
- It has stability and recoverability potential due to its magnetic property.

Chapter 5: The process optimisation and simple cost benefit analysis

This section presents modelling and optimisation of the integrated AD-AOP magnetized system for municipality wastewater treatment with estimated energy produced and CO_2 emission reduction. The process optimisation was needed to ascertain the key operating conditions of the integrated system for future implementation into a sustainable system.

5.1 Response surface methodology

In this work, which is an extension of previous findings, three input factors – organic loading rate (OLR), hydraulic retention time (HRT), and irradiation light source (visible, UV, and UV-vis) were evaluated, optimized, and modelled to provide four (4) distinct output variables. The outputs included biogas production, COD removal efficiency, bioenergy production (Ebio) and amount of energy consumed (Euv). Also, the system energy degree and CO_2 emission reduction was estimated based on the organic load degraded (%COD removal) per effect of the RSM-BBD experimental conditions (Table 9). This infers integrating of the AD and AOP to provide a sustainable alternative solution for offsetting the AOP energy demand with biogas produced by the AD system, while the magnetised system facilitates the recovery of Fe-TiO_2 nanoparticles. In terms of the energy analysis, the integrated system per unit wastewater treated was estimated based on the OLR (5.1) of the system.

$$OLR = \frac{Cf.Q}{V} \qquad (5.1)$$

where Cf is the feed concentration (kg COD/L), Q is the feed flow rate (L/d) and V is the reactor volume (L)

Table 9: Experimental design

Factors	Symbol	Low level (-1)	Centre points (0)	High level (+1)
OLR (kg COD/L.d)	A	0.394	0.85	1.3
HRT (d)	B	1	16	31
Light source (vis/UV-vis/UV)	C	Vis	UV-vis	UV

5.2 Data collection and response analysis

The AD biogas production was monitored daily using the downward-water displacement technique, where the cumulative biogas produced was estimated using the HRT assigned level (Table 9). The degree of degradability of the wastewater was estimated based on the %COD removal expressed in equation (5.2).

$$\%COD\ removal = \left(\frac{C_i - C_f}{C_i}\right) x\ 100 \qquad (5.2)$$

To estimate the energy produced by the AD process to offset the AOP electricity required for the photodegradation, the energy production by the AD process was calculated by equation (5.3) (Apollo et al., 2013).

$$Ebio = LHV_{CH_4} \times E_{COD} \times C_{COD} \times \alpha_{CH_4} \qquad (5.3)$$

Where $Ebio$ is the AD energy production (kWh/L), LHV_{CH_4} is the low heating value of methane, which is 10.55 kWh/m^3 (10.55×10^{-3} kWh/L) (Apollo et al., 2013). E_{COD} is the COD removal efficiency, C_{COD} is the feed concentration (kg COD/L) and α_{CH_4} is the methane production coefficient (L/kg COD removed). The energy consumption of the UV photodegradation process (EUV) was calculated using (5.4) (Apollo et al., 2013).

$$Euv = \frac{P.t}{V.log\left(\frac{Ci}{Cf}\right)} \tag{5.4}$$

Where P is the AOP lamp power consumption (kW), t is the irradiation time (hours), V is the volume (L) of water treated, and C_i and C_f are the initial and final concentrations of the target contaminant. Furthermore, the energy ratio (β), which is the efficiency indicator of the integrated system (AD-AOP) was calculated with equation (5.5)

$$\beta = \frac{Ebio}{Euv} \tag{5.5}$$

Where E_{UV} is the UV lamp energy consumption (kWh/L) and $Ebio$ is the bioenergy production (kWh/L).

The energy efficiency and environmental impact was estimated based on the conversion rate of the biomethane into electricity. This was estimated based on the assumed 78% of the energy produced, where 33% was electricity generated from the biogas and 45% was estimated as heat in a co-generation process (Apollo et al., 2016; Bella and Rao, 2021). Herein, the electricity potential (El_{bio}) can be expressed (5.6) as 33% of the total bioenergy generated per unit effluent volume treated (kWh/m^3). Also, the energy utilised by the pumps was approximated by equation (5.7).

$$El_{bio} = 0.33E_{bio} \tag{5.6}$$

$$Ep = \frac{Q\rho gh}{\omega} \tag{5.7}$$

where E_p is pump power (W), Q is the flow rate of the recycle stream (m^3/s), ρ is fluid density (kg/m^3), g is the gravitational acceleration (m/s^2), h is the head (m) and ω is the pump efficiency, which was assumed to be 0.6 (Abdullah et al., 2017; Mwakasonda & Winkler, 2015).

5.3. One-factor-at-time approach

5.3.1 Treatability efficiency

The integrated AD-AOP operating parameters were initially screened to determine the system's overall performance. Figure 11 shows the COD and Colour removal were within 75-80% and 50-60%, respectively for the AD-AN units. Conversely, the degree of colour reduction in the

AD-AN process was found to be not very efficient as compared to the AOP-MS system. Meanwhile, the post-treatment AOP-MS was able to increase the removal efficiency above 85-95%. Evidently, with the degree of colour and COD reduction (Figure 11) by the AOP-MS, the overall performance of the integrated system (AD-AN-AOP-MS) was found to be feasible. Therefore, integrating the AD-AOP system into the wastewater treatment settings is highly appreciable.

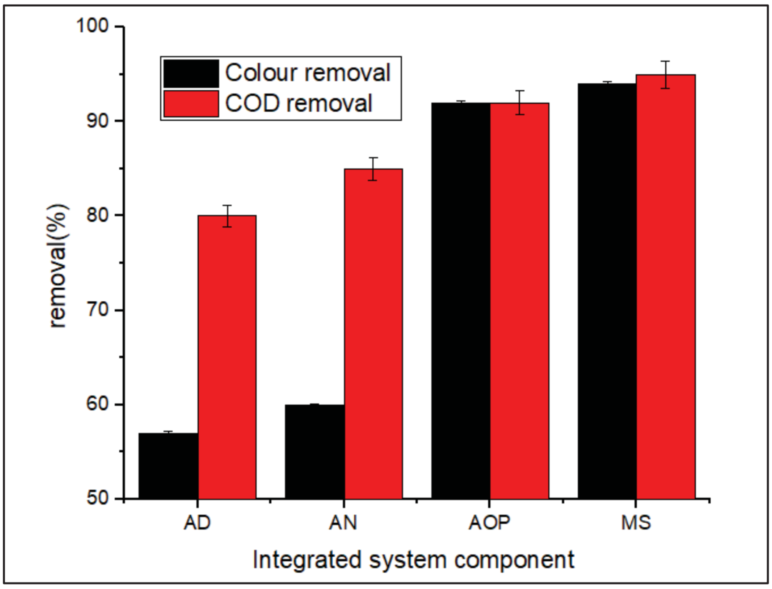

Figure 11: Removal of COD and Colour by the integrated system component units; AD-anaerobic digestion; AN-buffer system; AOP-advanced oxidation process; Ms-Magnetic filter system

5.3.2 Comparing photo-irradiation source

As photoactivation of Fe-TiO_2 are energy driven, three artificial light sources viz. visible (vis), ultraviolet-vis (UV-vis) and ultraviolet (UV) irradiation were investigated. All the light sources, being in photoactive wavelength range of $\lambda > 400$ nm, ignited the Fe-TiO_2 photons, which increased the photoactivity and neutralisation of the intermediate oxidation products. Figure 12 shows the correlated kinetic plots for the photodegradation of COD and colour with respect to the time.

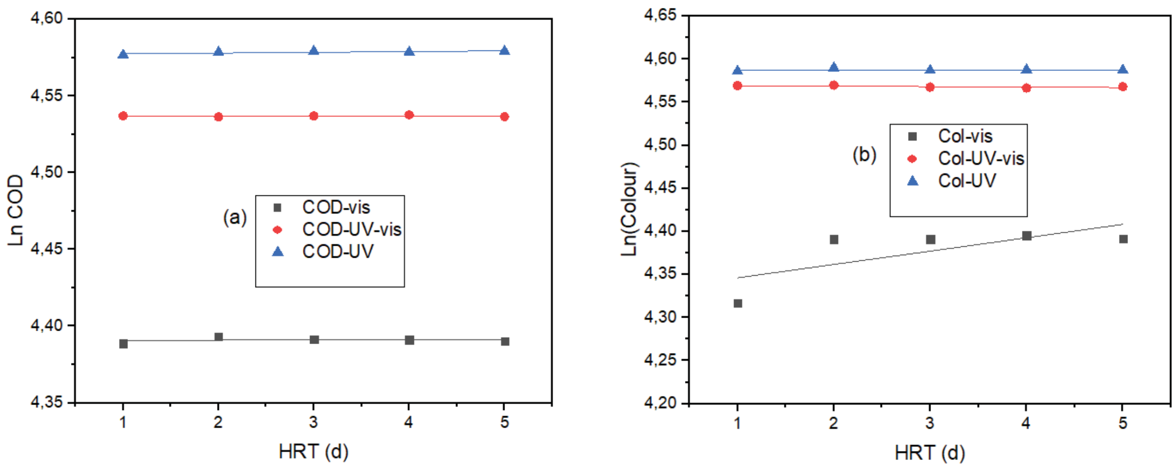

Figure 12: Pseudo-first order kinetic plot of (a) COD and (b) colour removal by the photo-intensity source

5.4 Response model development

The Box Behnken design (BBD) matrix was used to investigate the effect of the input variable on the process. With the randomised run order, input variable (OLR, HRT and light source) combinations were built via the Design Expert software (Version 13.0.7), whereas the responses (biogas produced, %COD removal, Ebio and Euv) were data experimentally generated via the integrated system (AD-AN-AOP-MS) monitoring. Table 10 presents the summary of response ranges with the ratio of minimum to maximum coupled with the mean and the standard deviation (Std Dev) values. This suggested the input variable had substantial effect on the response, even though some of the responded values were significantly exceptional.

Table 10: Statistical summary of the RSM-BBD responses

Response	Name	Units	Minimum	Maximum	Mean	Std. Dev.	Ratio
R1	Biogas	mL/d	250	1950	1078.33	615.20	7.80
R2	COD	%	95.84	99.90	97.84	1.38	1.04
R3	Ebio	kWh/L	24.30	143.73	43.34	28.78	5.92
R4	EUV	kWh/L	98.96	488.13	282.12	131.98	4.93

5.4.1 Response model studies

Correlated quadratic models expressed in equations (5.8-5.11) in their actual input factor levels were selected. The positive (+) and negative (-) signs of the coefficient elucidate the energetic and antagonistic effect of the input variables on the response.

$$Biogas_{actual}(Y_1) = 859.94 - 2209.8(OLR) + 70.51HRT + 161Light_{type} + 22.1(OLR * HRT) - 220.75(OLR * light_{type}) - 11.67(HRT * light_{type}) + 1258.879OLR^2 - 1.47HRT^2 + 283.3Light_{type}^2 \quad (5.8)$$

$$COD_{actual}(Y_2) = 97.74 - 0.36(OLR) + 0.061HRT + 1.59Light_{type} - 0.07(OLR * HRT) + 0.0036HRT^2 + 0.005(OLR * HRT^2) \quad (5.9)$$

$$Ebio_{actual}(Y_3) = 104.96 - 142.08(OLR) + 1.997HRT + 148.66Light_{type} - 14.07(OLR * HRT) - 277(OLR * light_{type}) + 80.5OLR^2 - 0.084HRT^2 + 129.19(OLR^2 * Light_{type}) + 0.0259(OLR * HRT^2) \quad (5.10)$$

$$Euv_{actual}(Y_3) = 421.01 - 169.18(OLR) + 15.42HRT - 128.86\, Light_{type} - 12.07(OLR * HRT) + 147.36(OLR * light_{type}) - 0.2835\,(HRT *\ Light_{type}) + 133.8OLR^2 - 0.193HRT^2 - 167.5\,(\,Light\_type^2) + 0.089(OLR * HRT^2) \quad (5.11)$$

5.4.2 Response optimisation and predictability

Using the response quadratic models, the RSM-BBD numerical optimisation technique was employed to maximise the system efficiency. At optimum conditions of OLR of 0.394 kg COD/Ld. and HRT of 20 days under UV-light intensity, a desirability of 75% was attained with maximum response shown in Table 11.

Table 11: Experimental validity of the RSM-BBD predicted results at optimal conditions

Solution 1 of 35 Response	Predicted Mean	Observed	Std Dev	SE Pred
Biogas (mL/d)	1279.73	1250	120.76	154.43
COD (%)	99.06	98.0	0.34	0.41
Ebio (kWh/L)	132.7	130	1.5	2
EUV (kWh/L)	304	302	1	1

5.4.3 Cost benefit analysis

The integrated system cost-benefits were estimated based on the sustainable energy production (biogas). As a bottom-line approach, the utilisation of wastewater resources for biogas production with reasonable environmental and social economic benefits warrant robust decentralised technologies. Herein, the integrated system concept provided a technical solution of improving the methane content of the AD biogas produced to subsidise the energy required by the UV-lamp (which is the major electric component of the AOP system). This was estimated based on the aforementioned optimum conditions obtained. As illustrated in Figure 13, the energy utilised by the AOP system is reduced when the AD-AOP system is integrated. This was found to be economically viable as reported by Apollo et al. (2013) findings.

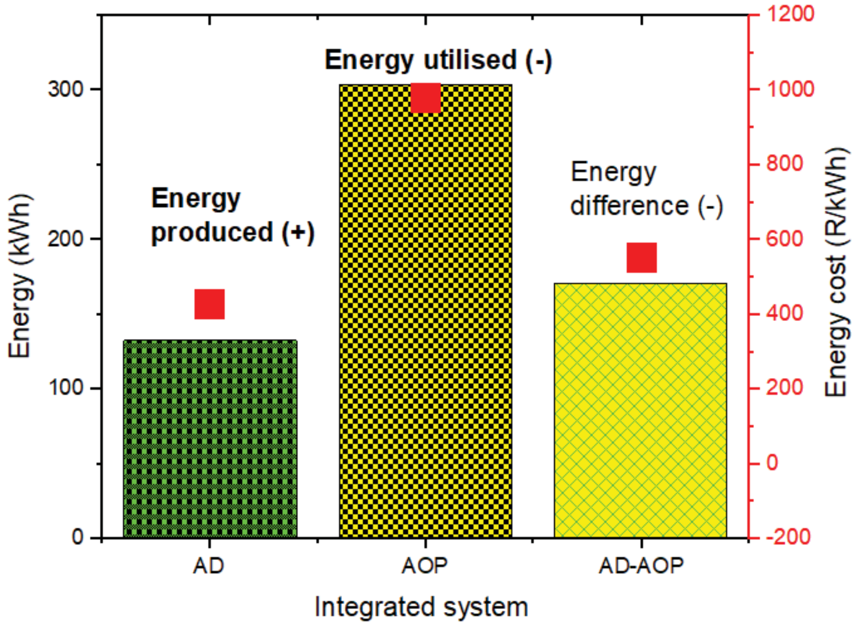

Figure 13: Energy estimated cost by applying electricity at a unit cost of R3.22 ($0.23) per kWh under the selected optimized condition

5.5 Summary

The integrated AD-photodegradation magnetised system developed was essentially a zero-waste system that made optimal use of the organic content of wastewater to produced biogas. Also, the synergetic integrated cycle of the system was observed as a profit-making process where the by-product of each process becomes the feedstock for another process. By using the RSM-BBD experimental matrices and response models, 75% desirable treatability efficiency was achieved at OLR of 0.394 kg COD/Ld and HRT of 20 days. The AD produced 132.7 kWh/L of energy while the UV light consumed 304.18 kWh/L. This means that the bioenergy produced might cover up to 60% of the energy required by the UV lamp to photodegrade 1 L of wastewater. The simple cost-benefit analysis showed a R979.46 ($69.96) reduction in electricity costs of the AOP system to R552.17 ($39.45) when the integrated system was used. Therefore, the prospects of AD bioenergy to subsidise the cost of UV photodegradation when combined in the wastewater settings was found to be economically viable.

Chapter 6: Conclusions and recommendations

6.1 Conclusion

This project aimed at developing an integrated anaerobic-photocatalytic (AD-AOP) magnetized system as a technological solution for wastewater treatment with bioenergy and sustainable environmental benefits.

- Among the magnetised – photocatalysts (MPCs) of binary (Fe-TiO_2) and ternary (Fe/Ch-TiO_2 and Fe/Al-TiO_2) synthesised, the Fe-TiO_2 with high surface area (62.73 m^2/g), pore volume (0.017 cm^3/g) and pore size (1.337 nm) was found to be the best for both wastewater treatment (>75% COD removal) and biogas enhancement (> 85% CH_4).
- The proof of concept showed the great potential of the MPCs to reduce the process time complexity in the AD process, toxicological effect of trace metals (27 elements considered), sludge production and additional usage of chemicals in the wastewater treatment system. Thus, the MPCs have separation and recoverability potential due to their stable and paramagnetic properties.
- At the RSM-BBD optimal conditions of 0.394 kgCOD/L. d OLR, 20 d HRT and AOP with UV-light irradiation, biogas of 1250 mL/d with 99% COD removal, 38.02 kWh/L bioenergy produced, 98.96 kWh/L UV energy used, a net energy efficiency of 38.43% and CO_2 emission reduction of 10859.5 kgCO_2e/L were estimated.

Above all, the prospect to upscale the current integrated system into a pilot- and large-scale unit with a smart-online monitoring system for wastewater treatment towards a sustainable environment was seen viable, hence should be given attention. In addition, magnetic photocatalysts (MPCs) with recoverability potentials for wastewater treatment were explored, whereby their applicability in magnetised coagulation, bioelectrolysis, biocatalysis and bioenergy can be explored.

6.2 Recommendation

As the scope of this current project was beyond the MPCs toxicological impact in microbial community shift and quantification, decontamination of specified emerging contaminants (phenols, antibiotics, pesticides, etc.), a detailed cost-benefit analysis and life cycle assessment necessitates further research work. Furthermore, advancing this novel integrated AD-AOP magnetised technology in the wastewater setting will be advantageous to industrial players and other stakeholders including:

- The upscaling of the integrated system into a smart online monitoring system for feasibility, technological evaluation and optimization will be useful to water engineers for wastewater treatment technology capacity development.
- The technological and scientific exploration for industrial adoption will assist in national/regional action plans and policies by the relevant decision-making stakeholders in the water sector to add value to the wastewater treatment.
- The recoverability potential of the MPCs for reuse will reduce the operational cost of the integrated system as well as mitigate the detrimental effect of trace elements complexity in the wastewater settings.

References

Abdulhameed, A. S., Mohammad, A.-T. and Jawad, A. H. 2019. Application of response surface methodology for enhanced synthesis of chitosan tripolyphosphate/TiO2 nanocomposite and adsorption of reactive orange 16 dye. *Journal of Cleaner Production*, 232: 43-56.

Ajay, C., Mohan, S., Dinesha, P. and Rosen, M. A. 2020. Review of impact of nanoparticle additives on anaerobic digestion and methane generation. *Fuel*, 277: 118234.

Álvarez, P. M., Jaramillo, J., Lopez-Pinero, F. and Plucinski, P. K. 2010. Preparation and characterization of magnetic TiO2 nanoparticles and their utilization for the degradation of emerging pollutants in water. *Applied Catalysis B: Environmental*, 100 (1-2): 338-345.

Amini, M., Rahimpour, A. and Jahanshahi, M. 2016. Forward osmosis application of modified TiO2-polyamide thin film nanocomposite membranes. *Desalination and Water Treatment* 57(30): 14013-14023. Available: https://doi.org/10.1080/19443994.2015.1065441 (Accessed 26 January 2021).

Apollo, S., Onyango, M. S. and Ochieng, A. 2013. An integrated anaerobic digestion and UV photocatalytic treatment of distillery wastewater. *Journal of Hazardous Materials*, 261: 435-442.

Apollo, S., Onyango, M. S. and Ochieng, A. 2016. Modelling energy efficiency of an integrated anaerobic digestion and photodegradation of distillery effluent using response surface methodology. *Environmental technology*, 37 (19): 2435-2446.

Appels, L., Baeyens, J., Degrève, J. and Dewil, R. 2008. Principles and potential of the anaerobic digestion of waste-activated sludge. *Progress in Energy and Combustion Science*, 34 (6): 755-781.

Askari, M. B. and Salarizadeh, P. 2020. Binary nickel ferrite oxide (NiFe2O4) nanoparticles coated on reduced graphene oxide as stable and high-performance asymmetric supercapacitor electrode material. *International Journal of Hydrogen Energy*, 45 (51): 27482-27491.

Ayers, M. R. and Hunt, A. J. 2001. Synthesis and properties of chitosan-silica hybrid aerogels. *Journal of Non-Crystalline Solids*, 285 (1-3): 123-127.

Bella, K. and Rao, P. V. 2021. Anaerobic digestion of dairy wastewater: effect of different parameters and co-digestion options—a review. *Biomass Conversion and Biorefinery*: 1-26.

Bourgin, M., Beck, B., Boehler, M., Borowska, E., Fleiner, J., Salhi, E., Teichler, R., von Gunten, U., Siegrist, H. and McArdell, C. S. 2018. Evaluation of a full-scale wastewater treatment plantupgraded with ozonation and biological post-treatments: Abatement of micropollutants, formation of transformation products and oxidation by-products. *Water Res*, 129: 486-498.

Dan Eddy, M. 2003. *Wastewater Engineering: Treatment, Disposal and Reuse*. 4th Edition ed. New York: Mc Graw Hill Book Co. Singapore.

De Clercq, D., Wen, Z., Gottfried, O., Schmidt, F. and Fei, F. 2017. A review of global strategies promoting the conversion of food waste to bioenergy via anaerobic digestion. *Renewable and Sustainable Energy Reviews*, 79: 204-221.

Debnath, S., Maity, A. and Pillay, K. 2014. Magnetic chitosan-GO nanocomposite: Synthesis, characterization and batch adsorber design for Cr (VI) removal. *Journal of environmental chemical engineering*, 2 (2): 963-973.

Dong, H., Zeng, G., Tang, L., Fan, C., Zhang, C., He, X. and He, Y. 2015. An overview on limitations of TiO_2-based particles for photocatalytic degradation of organic pollutants and the corresponding counter measures. *Water Research*, 79: 128-146.

Durán, I., Rubiera, F. and Pevida, C. 2021. Modeling a biogas upgrading PSA unit with a sustainable activated carbon derived from pine sawdust. Sensitivity analysis on the adsorption of CO_2 and CH4 mixtures. *Chemical Engineering Journal*: 132564.

El Ghandoor, H., Zidan, H., Khalil, M. M. and Ismail, M. 2012. Synthesis and some physical properties of magnetite (Fe3O4) nanoparticles. *Int. J. Electrochem. Sci*, 7 (6): 5734-5745.

Elhambakhsh, A., Zaeri, M. R., Mehdipour, M. and Keshavarz, P. 2020. Synthesis of different modified magnetic nanoparticles for selective physical/chemical absorption of CO_2 in a bubble column reactor. *Journal of environmental chemical engineering*, 8 (5): 104195.

Gao, H. and Zeng, D. L. 2003. Experimental investigation of intensified heat exchange based on selfexcited oscillating pulse jets. *Reneng Dongli Gongcheng/Journal of Engineering for Thermal Energy and Power*, 18 (4): 349-351+360.

Gao, X., Bi, J., Wang, W., Liu, H., Chen, Y., Hao, X., Sun, X. and Liu, R. 2020. Morphology-controllable synthesis of NiFe2O4 growing on graphene nanosheets as advanced electrode material for high performance supercapacitors. *Journal of Alloys and Compounds*, 826: 154088.

Gimeno, O., García-Araya, J. F., Beltrán, F. J., Rivas, F. J. and Espejo, A. 2016. Removal of emerging contaminants from a primary effluent of municipal wastewater by means of sequential biological degradation-solar photocatalytic oxidation processes. *Chemical Engineering Journal*, 290: 12-20.

Göbel, A., McArdell, C. S., Joss, A., Siegrist, H. and Giger, W. 2007. Fate of sulfonamides, macrolides, and trimethoprim in different wastewater treatment technologies. *Science of The Total Environment*, 372 (2): 361-371.

Goswami, R. K., Mehariya, S., Obulisamy, P. K. and Verma, P. 2021. Advanced microalgae-based renewable biohydrogen production systems: A review. *Bioresource Technology*, 320: 124301.

Guo, Q., Zhou, C., Ma, Z. and Yang, X. 2019. Fundamentals of TiO2 photocatalysis: concepts, mechanisms, and challenges. *Advanced Materials*, 31 (50): 1901997.

Kamal, M. A., Bibi, S., Bokhari, S. W., Siddique, A. H. and Yasin, T. 2017. Synthesis and adsorptive characteristics of novel chitosan/graphene oxide nanocomposite for dye uptake. *Reactive and functional polymers*, 110: 21-29.

Khodadadi, M., Al-Musawi, T. J., Kamani, H., Silva, M. F. and Panahi, A. H. 2020. The practical utility of the synthesis FeNi3@SiO2@TiO2 magnetic nanoparticles as an efficient photocatalyst for the humic acid degradation. *Chemosphere*, 239: 124723.

Kim, D. W., Enomoto, N., Nakagawa, Z. e. and Kawamura, K. 1996. Molecular dynamic simulation in titanium dioxide polymorphs: Rutile, brookite, and anatase. *Journal of the American Ceramic Society*, 79 (4): 1095-1099.

Kiser, M., Westerhoff, P., Benn, T., Wang, Y., Perez-Rivera, J. and Hristovski, K. 2009. Titanium nanomaterial removal and release from wastewater treatment plants. *Environmental science & technology*, 43 (17): 6757-6763.

Kobwittaya, K. and Sirivithayapakorn, S. 2014. Photocatalytic reduction of nitrate over Fe-modified TiO2. *APCBEE procedia*, 10: 321-325.

Kweinor Tetteh, E. and Rathilal, S. 2021. Biogas production from wastewater treatment-evaluating anaerobic and biomagnetic systems. *Water-Energy Nexus*, 4: 165-173.

Kyzas, G. Z., Travlou, N. A. and Deliyanni, E. A. 2014. The role of chitosan as nanofiller of graphite oxide for the removal of toxic mercury ions. *Colloids and Surfaces B: Biointerfaces*, 113: 467-476.

Lai, H., Xu, F. and Wang, L. 2018. A review of the preparation and application of magnetic nanoparticles for surface-enhanced Raman scattering. *Journal of Materials Science*, 53 (12): 8677-8698.

Lamichhane, N., Sharifabad, M. E., Hodgson, B., Mercer, T. and Sen, T. 2022. Superparamagnetic iron oxide nanoparticles (SPIONs) as therapeutic and diagnostic agents. In: *Nanoparticle Therapeutics*. Elsevier, 455-497.

Lin, B. and Sai, R. 2021. A multi factor Malmquist CO_2emission performance indices: Evidence from Sub Saharan African public thermal power plants. *Energy*, 223: 120081.

Liu, S., Yu, B., Wang, S., Shen, Y. and Cong, H. 2020. Preparation, surface functionalization and application of Fe3O4 magnetic nanoparticles. *Advances in Colloid and Interface Science*, 281: 102165.

Lu, A. H., Salabas, E. e. L. and Schüth, F. 2007. Magnetic nanoparticles: synthesis, protection, functionalization, and application. *Angewandte Chemie International Edition*, 46 (8): 1222-1244.

Malato, S., Fernández-Ibáñez, P., Maldonado, M. I., Blanco, J. and Gernjak, W. 2009. Decontamination and disinfection of water by solar photocatalysis: Recent overview and trends. *Catalysis Today*, 147 (1): 1-59.

Mecha, A. C., Onyango, M. S., Ochieng, A., Fourie, C. J. S. and Momba, M. N. B. 2016. Synergistic effect of UV-vis and solar photocatalytic ozonation on the degradation of phenol in municipal wastewater: A comparative study. *Journal of Catalysis*, 341: 116-125.

Mohammed, L., Gomaa, H. G., Ragab, D. and Zhu, J. 2017. Magnetic nanoparticles for environmental and biomedical applications: A review. *Particuology*, 30: 1-14.

Momba, M. and Swartz, C. D. 2010. Guidelines for the assessment of the compliance of South African potablewater supply with accepted drinking water quality standards and management norms. *WRC Report*, (425/10)

Paździor, K., Bilińska, L. and Ledakowicz, S. 2019. A review of the existing and emerging technologies in the combination of AOPs and biological processes in industrial textile wastewater treatment. *Chemical Engineering Journal*, 376

Popp, J., Lakner, Z., Harangi-Rákos, M. and Fári, M. 2014. The effect of bioenergy expansion: Food, energy, and environment. *Renewable and Sustainable Energy Reviews*, 32: 559-578.

Rezlescu, N., Rezlescu, E., Popa, P. D., Doroftei, C. and Ignat, M. 2014. Scandium substituted nickel-cobalt ferrite nanoparticles for catalyst applications. *Applied Catalysis B: Environmental*, 158: 70-75.

Riaz, S. and Park, S.-J. 2020. An overview of TiO2-based photocatalytic membrane reactors for water and wastewater treatments. *Journal of industrial and engineering chemistry*, 84: 23-41.

Rojo, E., Carmona, A., Soto, C., Díaz, I., Fernández-Polanco, M., Palacio, L., Muñoz, R. and Bolado, S. 2021. Environment and Material Science Technology for Anaerobic Digestion-Based Circular Bioeconomy. In: *Biomass, Biofuels, Biochemicals*. Elsevier, 25-55.

Russo, V. and Von Blottnitz, H. 2017. Potentialities of biogas installation in South African meat value chain for environmental impacts reduction. *Journal of Cleaner Production*, 153: 465-473.

Sahani, S., Sharma, Y. C. and Kim, T. Y. 2022. Emerging Contaminants in Wastewater and Surface Water. In: *New Trends in Emerging Environmental Contaminants*. Springer, 9-30.

Saiz, J., Bringas, E. and Ortiz, I. 2014. Functionalized magnetic nanoparticles as new adsorption materials for arsenic removal from polluted waters. *Journal of Chemical Technology & Biotechnology*, 89 (6): 909-918.

Sharma, R. K., Dutta, S., Sharma, S., Zboril, R., Varma, R. S. and Gawande, M. B. 2016. Fe3O4(iron oxide)-supported nanocatalysts: synthesis, characterization and applications in coupling reactions. *Green Chemistry*, 18 (11): 3184-3209.

Sivaranjanee, R. and Kumar, P. S. 2021. A review on remedial measures for effective separation of emerging contaminants from wastewater. *Environmental Technology & Innovation*, 23: 101741.

Son, D.-J., Kim, W.-Y., Jung, B.-R., Chang, D. and Hong, K.-H. 2020. Pilot-scale anoxic/aerobic biofilter system combined with chemical precipitation for tertiary treatment of wastewater. *Journal of Water Process Engineering*, 35: 101224.

Suzuki, H., Araki, S. and Yamamoto, H. 2015. Evaluation of advanced oxidation processes (AOP) using O3, UV, and TiO_2 for the degradation of phenol in water. *Journal of Water Process Engineering*, 7: 54-60.

Thakre, K. G., Barai, D. P. and Bhanvase, B. A. 2021. A review of graphene-TiO2 and graphene-ZnO nanocomposite photocatalysts for wastewater treatment. *Water Environment Research*, 93 (11): 2414-2460.

Van Niekerk, A. and Schneider, B. 2013. Implementation plan for direct and indirect water re-use for domestic purposes-Sector discussion document. *Water Research Commission Report KV*, 320: 13.

Watson, S., Beydoun, D. and Amal, R. 2002. Synthesis of a novel magnetic photocatalyst by direct deposition of nanosized TiO2 crystals onto a magnetic core. *Journal of Photochemistry and Photobiology A: Chemistry*, 148 (1-3): 303-313.

Xu, L., Niu, J., Xie, H., Ma, X., Zhu, Y. and Crittenden, J. 2021. Effective degradation of aqueous carbamazepine on a novel blue-colored TiO2 nanotube arrays membrane filter anode. *Journal of Hazardous Materials*, 402: 123530.

Zhao, J., Li, Y. and Dong, R. 2021a. Recent progress towards in-situ biogas upgrading technologies. *Science of The Total Environment*, 800: 149667.

Zhao, T., Qian, R., Zhou, G., Wang, Y., Lee, W. I. and Pan, J. H. 2021b. Mesoporous WO3/TiO2 spheres with tailored surface properties for concurrent solar photocatalysis and membrane filtration. *Chemosphere*, 263: 128344.